frontiers in Marine Science

ORIGINAL RESEARCH
published: 18 August 2021
doi: 10.3389/fmars.2021.699483

Environmental Factors Affecting Spatial Dinoflagellate Cyst Distribution in Surface Sediments Off Aveiro-Figueira da Foz (Atlantic Iberian Margin)

Iria García-Moreiras[1], Anabela Oliveira[2], Ana I. Santos[2,3], Paulo B. Oliveira[4] and Ana Amorim[5,6]*

[1] Basan Group, Centro de Investigación Mariña (CIM), Departamento de Bioloxía Vexetal e Ciencias do Solo, Facultade de Ciencias, Universidade de Vigo, Vigo, Spain, [2] Marine Geology Division, Instituto Hidrográfico (IH), Lisbon, Portugal, [3] Instituto Dom Luiz, Faculdade de Ciências, Universidade de Lisboa, Lisbon, Portugal, [4] Instituto Português do Mar e da Atmosfera (IPMA), Algés, Portugal, [5] Departamento de Biologia Vegetal, Faculdade de Ciências, Universidade de Lisboa, Lisbon, Portugal, [6] Centro de Ciências do Mar e do Ambiente (MARE), Faculdade de Ciências, Universidade de Lisboa, Lisbon, Portugal

OPEN ACCESS

Edited by:
Janine Barbara Adams, Nelson Mandela University, South Africa

Reviewed by:
Gustaaf Marinus Hallegraeff, University of Tasmania, Australia
Sofia Ribeiro, Geological Survey of Denmark and Greenland, Denmark

***Correspondence:**
Iria García-Moreiras
iriagamo@uvigo.es

Specialty section:
This article was submitted to Marine Ecosystem Ecology, a section of the journal Frontiers in Marine Science

Received: *23 April 2021*
Accepted: *05 July 2021*
Published: *18 August 2021*

Citation:
García-Moreiras I, Oliveira A, Santos AI, Oliveira PB and Amorim A (2021) Environmental Factors Affecting Spatial Dinoflagellate Cyst Distribution in Surface Sediments Off Aveiro-Figueira da Foz (Atlantic Iberian Margin). Front. Mar. Sci. 8:699483. doi: 10.3389/fmars.2021.699483

Resting cysts of planktonic dinoflagellates, once produced, sink to the seabed where they can remain viable for a long time. These cysts have important ecological roles, such as acting as the inoculum for the development of planktonic populations. Moreover, dinoflagellate cyst records from depth sediment cores are broadly used as a proxy to infer past environmental conditions. In this study, the main objective was to obtain information on the relationships between the spatial distribution of modern dinoflagellate cysts and present-day hydrography in the NW Iberian shelf. Cyst assemblages were analyzed in 51 surface sediment samples with varying grain sizes, collected at different water depths, following nine transects perpendicular to the coast, between Aveiro and Figueira da Foz (Atlantic Iberian margin). Multivariate statistical analyses revealed marked land-sea and latitudinal gradients in the distribution of cysts, and helped investigate how environmental factors [water depth, grain size, sea-surface temperature (SST), sea-surface salinity (SSS), bottom temperature (BTT) and surface chlorophyll-a concentration (CHL)] influence modern dinoflagellate cyst composition and abundances. Three main ecological signals were identified in the modern dinoflagellate cyst assemblages: (1) the heterotroph signal as the main upwelling signal; (2) the dominance of *P. reticulatum* and *L. polyedra* signal, indicative of warm stratified conditions, possibly reflecting transitional environments between more active inshore upwelling and warmer offshore waters; and (3) the *G. catenatum* signal for the presence of mid-shelf upwelling fronts. The almost absence of viable cysts of the toxic and potentially toxic species *G. catenatum L. polyedra* and *P. reticulatum* suggests that in the study area, for these species, there is no build-up of significant cyst beds and thus planktonic populations must depend on other seeding processes. These results are the

first detailed modern distribution of dinoflagellate cysts in the NW Iberian Atlantic margin (off Portugal), and show a good correspondence with hydrographic features of summer upwelling season in the study area, meaning that they are reflecting water column characteristics and therefore may be used as supporting evidence for the interpretation of stratigraphic cyst records and reconstruction of past marine ecosystems in W Iberia.

Keywords: dinoflagellate cysts, sediments, spatial distribution, environmental gradients, coastal ecosystems, HABs, Atlantic Iberian margin

INTRODUCTION

Dinoflagellates are a highly diverse group of protists that along with diatoms and coccolithophores are one of the most abundant groups of coastal marine phytoplankton, significantly contributing to primary productivity (Falkowski and Knoll, 2007). As a group, dinoflagellates present different trophic strategies: some are autotrophs (photosynthetic), others heterotrophs, but most of them are mixotrophic (able to combine both trophic modes) (Schnepf and Elbrächter, 1992; Hansen, 2011; Stoecker et al., 2017). The trophic strategy and life cycle traits together with different environmental preferences determine the ecology of the different species (Hansen, 2011).

Around 13–16% of living dinoflagellate species are known to form benthic resting stages (cysts) as part of their life-cycle (Head, 1996). Since then, several new species have been described and their cyst-theca relationship established (e.g., Luo et al., 2019). Once formed, cysts are accumulated in the bottom sediments where they can remain viable for a long time, playing important ecological roles. Benthic resting cysts are key for the survival of the species, acting as overwintering stages, inoculum for the formation of planktonic blooms or as a genetic reservoir (Anderson et al., 2005; Lundholm et al., 2011; Bravo and Figueroa, 2014; Ellegaard and Ribeiro, 2018). In the present-day warming scenario, recent work has highlighted the importance of considering cyst physiology when investigating the response of cyst forming dinoflagellates to environmental change (Brosnahan et al., 2020).

Given their capacity to fossilize, dinoflagellate cyst records from sediment cores are broadly used as a proxy to infer past environmental conditions (see Ellegaard et al., 2017 for a review). Stratigraphic cyst records, and more recently ancient DNA (De Schepper et al., 2019), represent a very valuable tool to study past biodiversity and reconstruct past marine ecosystems. However, interpretations of the cyst record can be biased by several factors related to the variable representation of the planktonic populations in the sediments. Importantly, post-depositional processes such as sediment reworking, horizontal transport and selective degradation of cysts (e.g., Zonneveld and Brummer, 2000; Zonneveld et al., 2018) can complicate the interpretation of the environmental signals (Ellegaard et al., 2017). Moreover, when inferring palaeoenvironmental data from cyst records we must consider that (1) not all dinoflagellate species produce resting cysts – i.e., they will not be represented in the cyst records – and (2) cyst productivity rates can vary between species – meaning some species can be over- or underrepresented in the sediment cyst record. Certain studies provide data which may help in overcoming these limitations, such as studies on cyst-theca relationships and cyst production dynamics (e.g., Susek et al., 2005; Bringué et al., 2013; Matsuoka and Head, 2013), and particularly those oriented to explore the relationships between modern cyst distributions in surface sediments and environmental gradients (e.g., Wall et al., 1977; Dale, 1996; Pospelova et al., 2008; Zonneveld et al., 2009; de Vernal et al., 2020; Van Nieuwenhove et al., 2020). Although a huge effort has been made to document in the Northern hemisphere the distribution of dinoflagellate cysts in surface sediments and their relation to major environmental variables [see Van Nieuwenhove et al. (2020) for an historical review] there are not many studies that investigate at a regional scale dinoflagellate cyst assemblages and their relation to present day hydrography, particularly coastal ecosystems of the Atlantic Iberian margin are still largely underrepresented in reference datasets (de Vernal et al., 2020).

Several dinoflagellates are responsible for harmful algal blooms (HAB) events, many of which produce resting cysts. These events can be associated with various threats in coastal systems, such as seafood poisoning or water discoloration (Hallegraeff et al., 2003). The W Iberian coast is frequently affected by these blooms which raise important economic and health safety concerns (Vale et al., 2008). In this region, within cyst producing HAB species, *Gymnodinium catenatum* is of particular concern given its association with the human syndrome Paralytic Shellfish Poisoning (PSP). Blooms of *G. catenatum* have been recorded in the West Iberian margin since late 1970s of the last century (Fraga et al., 1988), and since then have been thoroughly studied. These blooms are characterized by a high decadal and annual unpredictability. The conditions leading to bloom seeding and initiation are still not fully understood, although seeding from planktonic populations is considered the most plausible hypothesis (Fraga et al., 1993; Moita et al., 1998; Sordo et al., 2001; Amorim et al., 2004; Bravo et al., 2010; Smayda and Trainer, 2010). Blooms generally occur during the summer upwelling season in relation to upwelling-relaxation-downwelling cycles and the autumn upwelling-downwelling transition (Fraga et al., 1993; Moita et al., 1998; Pitcher et al., 2010). Upwelling plumes are important features on the dynamics of *G. catenatum* blooms. Moita et al. (2003) related the presence of *G. catenatum* in the inshore side of the upwelling plume front with the asymmetric hydrodynamic conditions of upwelling plumes rooted at major capes in the W Iberian coast. The presence of *G. catenatum* in frontal zones and downwelling conditions has been attributed to its high swimming velocities as a result of the long chain life-form strategy that characterizes this species (Fraga et al.,

1988; Moita et al., 2003; Pitcher et al., 2010). Evidence from the sub-fossil cyst record suggests this species recently colonized the NE Atlantic possibly by geographical range expansion from NW Africa (Ribeiro et al., 2012).

Lingulodinium polyedra (=*L. machaerophorum*) and *Protoceratium reticulatum* [=*Operculodinium centrocarpum* sensu Wall and Dale (1966)] are two other cyst-forming species of concern because of the production of a group of potentially nuisance toxins, the yessotoxins. *Lingulodinium polyedra* is also known to cause water discoloration in W and SW Iberia (Amorim et al., 2001, 2004), with high negative impacts on tourism. Blooms have been reported in summer and early autumn associated with warm stratified conditions (∼17°C) in the inshore side of nutrient rich upwelling filaments (Amorim et al., 2001, 2004). On a global scale, blooms of *L. polyedra* have been reported from temperate regions since the beginning of last century, occurring in summer-early fall (Lewis and Hallett, 1997). In the NE Atlantic, the distribution of *L. polyedra*, based on surface sediment cyst distributions, spans from the equatorial zone to the temperate/sub-polar boundary with a distribution center in NW Africa and the Gulf of Cadiz (Dale, 1996; Lewis and Hallett, 1997; Zonneveld et al., 2013; de Vernal et al., 2020).

Regarding *Protoceratium reticulatum*, very little is known on the ecology of the planktonic stage in this area, with only few records reported in phytoplankton studies off Portugal (Moita et al., 1998; Loureiro et al., 2011; Silva et al., 2015). In contrast, the cyst record in modern and subfossil sediments from the Atlantic Iberian margin, particularly in the NW Iberian coast, is characterized by the common occurrence of cysts of *P. reticulatum* – and also of *G. catenatum* and *L. polyedra* – (e.g., Amorim, 2001; Amorim et al., 2004; Sprangers et al., 2004; Ribeiro and Amorim, 2008; Ribeiro et al., 2016; García-Moreiras et al., 2015, 2018). Based on surface sediment cyst distributions, *P. reticulatum* is one of the most cosmopolitan species (e.g., Wall et al., 1977; Dale, 1996; Zonneveld et al., 2013). The proportional increase of this species (=*Operculodinium centrocarpum*) in cyst assemblages seems to be associated with unstable transitional conditions such as the neritic-oceanic boundary or the influence of river plumes (Dale, 1996; Dale et al., 2002).

Investigating the oceanographic mechanisms that control bloom dynamics of these and other HAB species is essential for the development of HAB forecasting tools and coastal monitoring programs (Wells et al., 2015; Berdalet et al., 2017). In this context, the study of dinoflagellate cyst distribution patterns in recent sediments and of the overlaying abiotic conditions is particularly interesting to understand how cysts can work as environmental proxies, identify the presence of potential cyst beds and detect rare species (Blanco, 1995; Dale, 1996; Orlova et al., 2004; Anderson et al., 2005; Ellegaard et al., 2017).

In this study, modern dinoflagellate cyst assemblages (concentration and relative abundance) and grain-size were analyzed in 51 surface sediment samples off Aveiro-Figueira da Foz (Atlantic Iberian margin). The well documented hydrography of the study area (Relvas et al., 2007; Oliveira et al., 2019) allowed the investigation of how well the cyst assemblages reflected the water column characteristics. The relationships between environmental variables – grain-size, water depth, sea-surface temperatures (SST), sea-surface salinities (SSS), bottom temperatures (BTT) and chlorophyll-a concentration (CHL) – and community composition were investigated by multivariate statistics to study how environmental gradients affect the present-day spatial distribution of dinoflagellate cysts. This work represents the first detailed dataset on modern dinoflagellate cyst distributions on the NW Portuguese shelf strongly influenced by seasonal upwelling, and may provide reference data for the interpretation of environmental signals from stratigraphic dinoflagellate cyst records to reconstruct past marine ecosystems in coastal environments from related or similar areas.

MATERIALS, DATA AND METHODS

Study Area

The sampling area is located between the latitudes 40°7′ and 40°49′ N and the longitudes −8°44′ and −9°18′ W, offshore Figueira da Foz-Aveiro (Iberian Atlantic margin) (**Figure 1A**). From south to north, the main freshwater sources in the study area are the Mondego river and the Ria de Aveiro (**Figure 1B**). The Mondego river has a catchment basin of 6670 km^2 and an annual average runoff of 500 m^{3}s^{-1} (Cunha and Dinis, 2002; Marques et al., 2002). Several rivers drain to the Ria de Aveiro – an estuary with coastal lagoon characteristics – with a total catchment area of ∼3600 m^2, Vouga being the largest river, with an average runoff of 29 m^{3}s^{-1} (Dias et al., 1999; Da Silva and Oliveira, 2007). Moreover, during periods of upwelling favorable winds, the study area may also be influenced by the Douro river plume, whose outlet is situated ∼35 km north of the study site (Fernández-Nóvoa et al., 2017). The Douro river has a larger catchment basin (98 073 km^2) and a mean discharge of 700 m^{3}s^{-1}, with a significant sediment load to the NW Iberian shelf (Dias et al., 2002; Oliveira et al., 2002; Fernández-Nóvoa et al., 2017).

Seasonal upwelling (spring-early autumn) and the variation of low-salinity buoyant plumes are among the main oceanographic features affecting the phytoplankton dynamics within the study area (Fiúza et al., 1982; Peliz et al., 2002; Moita et al., 2003; Oliveira et al., 2019). Latitudinal and onshore-offshore environmental gradients (e.g., SST, SSS) have been described during upwelling events, and sub-mesoscale oceanographic processes were suggested as major factors affecting the horizontal distributions of chlorophyll-a and biota (Moita, 2001; Oliveira et al., 2019).

In summer, the mean Chl-a and SST distributions have a typical coastal upwelling pattern: a coastal band of high Chl-a coinciding with low SST, resulting from the upwelling of cold, nutrient-rich, sub-surface waters. The resulting gradient is not uniform and usually presents a maximum at some distance from the coast along the so-called upwelling fronts. The distribution of the SST fronts in the study area have been studied by Relvas et al. (2007) who showed that these fronts are most frequently located around the 50 isobath, and identified a low frontal probability zone at mid-shelf (**Figure 1C**).

TABLE 1 | Samples studied in this paper and the six environmental parameters included in statistical analyses.

Sample label	Water depth (−m)	Grain size (mm)	SST (°C)	BTT (°C)	SSS	Chl-a ($\mu g.L^{-1}$)
B91	15.50	0.20	18.3	14.35	33.36	1.99
B67	28.50	0.15	18.3	13.84	34.66	1.53
B68	54.30	0.23	18.5	13.51	35.25	0.84
B69	84.70	0.16	18.6	13.26	35.36	0.61
B66	40.40	0.21	18.3	13.85	34.37	1.56
B65	62.10	0.19	18.5	13.50	35.24	0.82
B64	86.60	0.12	18.7	13.16	35.34	0.59
B63	102.20	0.08	18.8	12.94	35.39	0.47
B83	111.90	1.20	18.9	12.86	35.40	0.43
B82	117.80	0.19	18.9	12.79	35.39	0.40
B90	21.20	0.16	18.2	14.20	34.70	2.17
B49	45.10	0.31	18.3	13.66	35.06	1.37
B50	64.30	0.20	18.5	13.39	35.28	0.77
B51	87.60	0.12	18.7	13.09	35.33	0.57
B79	97.20	0.09	18.7	12.88	35.34	0.53
B89	16.50	0.15	18.2	13.99	34.85	2.28
B48	36.90	0.72	18.2	13.72	35.07	1.64
B47B	59.20	1.06	18.4	13.34	35.25	0.89
B46	72.80	0.21	18.6	13.13	35.32	0.65
B45	100.00	0.12	18.7	12.88	35.36	0.51
B78	113.70	0.10	18.7	12.74	35.38	0.45
B44	117.60	0.11	18.8	12.72	35.39	0.42
B88	16.20	0.65	18.1	14.04	34.82	2.58
B31	33.30	0.88	18.2	13.60	35.13	1.67
B32	51.70	1.18	18.3	13.34	35.23	1.02
B35	119.80	0.06	18.1	12.70	35.37	0.43
B87	18.70	0.12	18.1	13.97	34.73	2.47
B30	34.80	1.22	18.2	13.61	35.09	1.78
B29	54.20	1.52	18.3	13.30	35.17	0.96
B28	72.90	1.60	18.4	13.09	35.24	0.69
B27	90.40	0.21	18.5	12.86	35.34	0.52
B86	20.70	0.16	18.1	13.75	34.89	2.15
B16	37.10	1.78	18.2	13.52	35.07	1.59
B17	54.50	1.89	18.3	13.23	35.14	0.96
B18	75.00	1.42	18.4	12.99	35.23	0.69
B19	92.90	0.22	18.5	12.77	35.33	0.52
B76	111.70	0.81	18.5	12.65	35.37	0.45
B77A	127.70	0.22	18.6	12.64	35.38	0.42
B85	16.80	0.71	18.1	13.75	34.84	2.38
B15	34.80	1.91	18.1	13.53	35.01	1.37
B14	49.40	1.87	18.2	13.34	35.06	0.97
B13	70.30	1.43	18.3	13.05	35.18	0.71
B12	94.10	0.21	18.4	12.75	35.29	0.52
B11	128.70	0.14	18.4	12.63	35.38	0.42
B84	17.00	0.16	18.0	13.62	34.75	2.09
B1	31.00	0.97	18.1	13.48	34.87	1.47
B2	42.50	1.32	18.1	13.34	35.01	1.03
B3	61.30	2.20	18.2	13.02	35.16	0.80
B4	87.00	0.26	18.2	12.75	35.28	0.58
B5	118.00	0.63	18.3	12.61	35.35	0.46
B75	117.80	0.11	18.3	12.61	35.35	0.46
Mean	66.99	0.63	18.38	13.26	35.12	1.05
SD	35.71	0.63	0.24	0.46	0.35	0.66

SST, satellite-derived sea-surface temperature (average of the warmest trimester, July to September); BTT, sea-bottom temperature (average for the warmest trimester, July to September); SSS, sea-surface salinity (global median); Chl a, satellite-derived surface chlorophyll a concentration (global median). SST and Chl a concentration are satellite-derived parameters calculated from daily values from 2003 to 2019. BTT and SSS were determined by numerical models from a data series corresponding to the period 2018–2020 (for more details see the methods section of this paper). Mean and Standard Deviation (SD) are shown in the bottom rows.

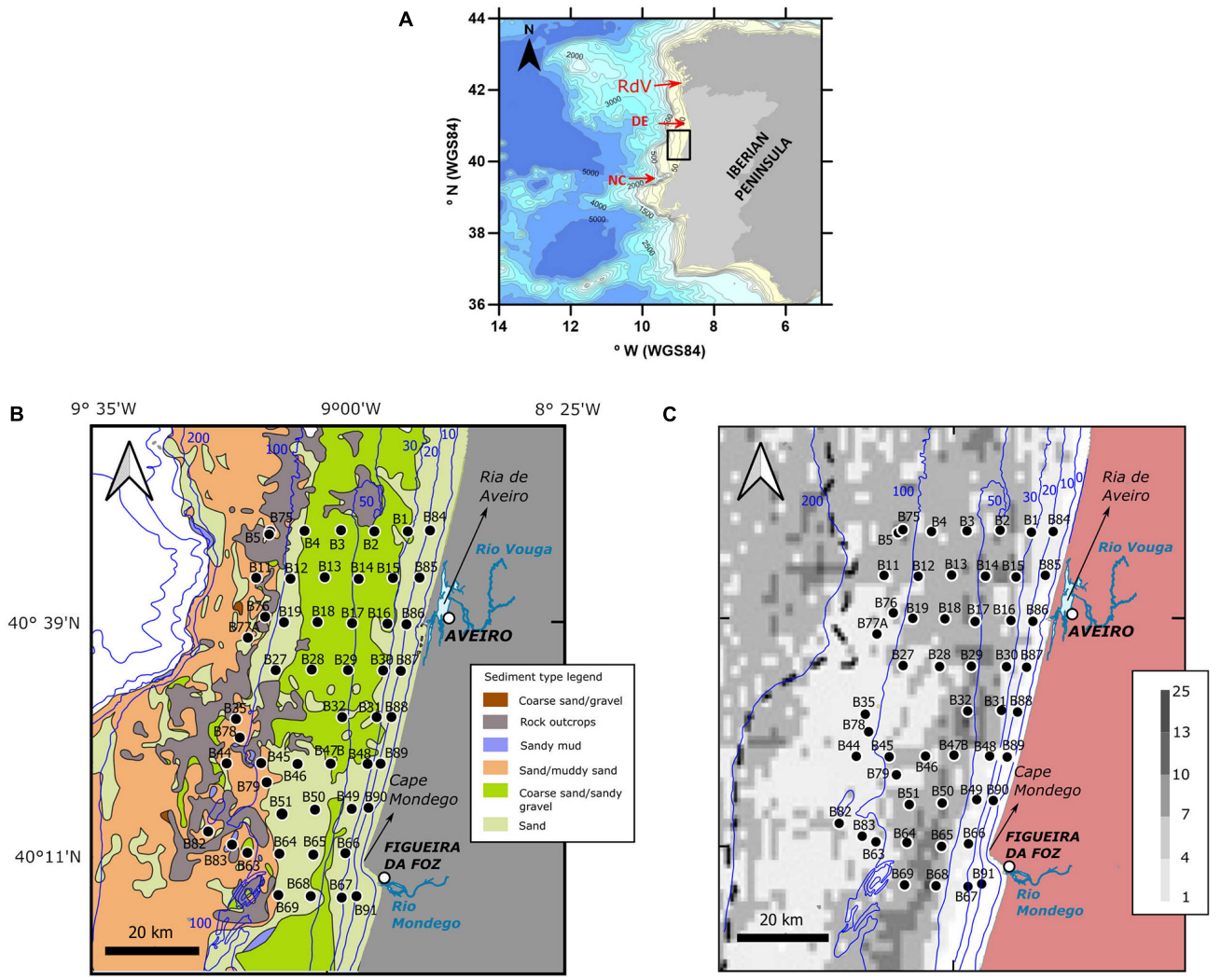

FIGURE 1 | Study site and location of sampling stations off Aveiro-Figueira da Foz (Atlantic Iberian margin). Red arrows **(A)** indicate the position of the Douro estuary (DE) and the Nazaré canyon (NC). Station positions **(B,C)** are superimposed on the Seabed Substrate maps from EMODnet Geology (https://www.emodnet-geology.eu/map-viewer/?p=seabed_substrate) **(B)** and the frontal probability map performed by Relvas et al. (2007) from average SST anomalies (°C) of satellite-derived summer data for the period 2001–2005 **(C)**. Bathymetric contours are in meters and are taken from the General Bathymetric Chart of the Oceans (https://www.gebco.net/) **(A)** and the IH (https://www.hidrografico.pt/op/33) **(B,C)**.

In the same area, Oliveira et al. (2019) described the bifurcation of the equatorward alongshore flow of upwelled waters originating further north (from 41–42°N) and the presence of a cyclonic area over the mid-shelf (~100 m isobath) (see their Figure 10) with a location that coincides with the low frontal probability zone of Relvas et al. (2007). SSS distribution is influenced by the low-saline waters of the Western Iberia Buoyant Plume (WIBP), composed mainly by freshwater loads from the Douro River (**Figure 1A**). During strong upwelling events, the WIBP is advected equatorward and covers most of the northern portion of the study area (Oliveira et al., 2019), with SSS increasing southwards and offshore.

During winter the predominant SW winds induce poleward currents along the shelf. However, winter upwelling events may be recorded generating equatorward currents (Relvas et al., 2007). Moita (2001) recorded short pulses of upwelling in the study area in winter, but these were not persistent enough to break the halo stratification at the surface induced by the well-developed buoyant low salinity plume. It is within these low salinity plumes that the low winter Chl-a maxima were recorded (Moita, 2001).

In the study area, the spatial distribution of the bottom sediments is influenced by bottom topography, river inputs and coastal hydrodynamics. The topography of the study region is characterized by a wide continental shelf with isobaths almost parallel to the coast (**Figures 1A,B**). The coast has no major protrusions except for Cape Mondego, where a persistent upwelling filament has been reported to occur during the upwelling season (Sousa and Bricaud, 1992). Fine sedimentary deposits are associated with rocky outcrops, which act as a barrier to the cross-shelf movement of sediment and also to

the general circulation (Oliveira et al., 2001). Latitudinally, two main circulation patterns affecting sediment distribution may be identified. In summer, higher intensity and frequency of upwelling promotes sediment transport southwards and offshore. In winter, when precipitation and storms are more intense and frequent, increased riverine supplies promote the transport of resuspended fine materials northwards (Fiúza et al., 1982; Fiúza, 1983; Vitorino, 1989).

Field Sampling

During the Hydrographic Institute of Portugal (IH)/AQUIMAR Cruise (March 2019), 51 surface sediment samples were collected with a Smith-McIntyre grab in coastal environments between the Ria de Aveiro and the Mondego (Figueira da Foz) outlets (**Figure 1**). Sampling stations followed nine land-sea transects perpendicular to the coast, corresponding to different grain-sizes and water depths (**Table 1**). For dinoflagellate cyst analyses, plexiglass tubes (3.6 cm internal diameter) were inserted in the sediment and the top 1-cm layer was collected and stored at 4°C in the dark for further analysis in the laboratory. For sediment characterization, the bulk grab sample, representative of the top 20 cm of surface sediment coverage, was collected and frozen (−18°C) until further analysis.

Laboratory Procedures

Grain-Size Analyses

In the laboratory, grain-size analyses were performed following the NP EN 933-1:2014 and ISO 13320:2009 standards (International Organization for Standardization [ISO], 2009; NP EN933-1, 2014). After sediment sample homogenization, splitting and salt and organic matter removal (using hydrogen peroxide, 30–130 volumes), grain-size analysis was performed combining two different methods: sieving (>500 μm) and laser diffraction (<500 μm) using a Malvern Mastersizer Hydro 2000, resulting in a continuous grain-size distribution curve in 0.5 φ intervals [$\varphi = -\log_2(D)$, where D = particle diameter in mm]. Grain size class dimensional limits were defined according to Wentworth (1922), modified by Dias (2004). Texture composition was classified according to Shepard (1954) in: gravel (diameter > 2 mm), sand (2–0.0625 mm), silt (0.0625–0.004 mm) and clay (<0.004 mm). Grain size statistics (mean, mode, standard deviation/sorting and asymmetry) were calculated according to Folk (1974) and McMannus (1988).

Sediment Processing for Dinoflagellate Cyst Analyses

A replicate of each sample (2 to 30 cm^3, depending on cyst concentration) was taken for dinoflagellate cyst analyses, which included wet-sieving with distilled water through a 150 μm-Nylon mesh and a 20 μm-stainless steel mesh (Endeccots) after sonication (60 s) (Elmasonic S50R). The retained fraction (between 150 and 20 μm) was centrifuged at 3600 rpm (∼2510 × *g*) (Eppendorf 5804 R), and the supernatant was then removed, and dinoflagellate cysts were further concentrated by centrifuging the homogenized pellet at 1000 rpm (∼190 × *g*) in a high-density solution of sodium polytungstate (∼2. 016 g cm^{-3}) (Bolch, 1997; Amorim et al., 2001). The floating organic fraction was collected, rinsed twice by centrifugation at 3600 rpm (∼2510 × *g*) (Eppendorf 5804 R) and recovered with filtered seawater in a final volume of 1 to 10 ml, depending on cyst concentration. Replicated sediment samples were used for dry weight determination (drying at 60°C until constant weight) and % moisture. The sample dry weight was determined using the previously calculated % moisture.

An inverted light microscope (Leica DMi1) was used for cyst counting and identification under 200x and 400x magnifications. One or more Sedgewick-Rafter chambers (1 ml) (Graticules Optics, United Kingdom) were counted to obtain a minimum of 100 cysts when possible, including both empty and cysts with cell contents (referred as full cysts onward), with an average of 264 cysts per sample. This method was used to obtain relative (percentage values of the total cyst assemblage) and absolute abundances. The latter were determined relative to the volume (cysts· ml^{-1}) and dry weight (cysts·g^{-1}) (**Supplementary Tables 1, 2**). Phase-contrast morphological examination (and photography) of some specimens were performed on a Zeiss Axiovert 200 microscope. All photographs (both bright-field and phase-contrast) were taken with a Zeiss Axiocam HRc camera. Finally, to keep a permanent collection as a backup, aliquots of all samples were mounted on slides using glycerine jelly and sealed with wax.

Notes on the Identification and Nomenclature of Dinoflagellate Cysts

The identification and nomenclature of dinoflagellate cysts follow Zonneveld and Pospelova (2015), Gurdebeke et al. (2019), Mertens et al. (2020), and Van Nieuwenhove et al. (2020). When species-level identification was not possible, the identification was done at the genus or higher level. The biological names were used preferentially, however, in those cases where the cyst-theca relationship is not clear, the paleontological name was used instead (e.g., *Quinquecuspis concreta*; see **Table 2**). This was also applied in the cases when the name refers to one of various cyst (morpho)types that are currently linked to only one species (e.g., *Votadinium calvum*, which illustrates one cyst type of *Protoperidinium oblongum*).

Unidentifiable spiny brown cysts were grouped as "spiny brown cysts" or SBC (**Table 2**) for data analysis purposes and inter-sample cyst-record comparison, due to some common difficulties with their identification (see Radi et al., 2013). Unidentifiable Round Brown cysts (RBC) included folded and broken round brown cysts that were not assigned to any specific genera (probably *Brigantedinium* sp., *Dubridinium* sp., etc.), and also specimens of *Diplopsalis*-type (**Table 2**). The latter includes light brown to grayish round cysts, with smooth surface and theropylic archeopyle, which correspond to cysts of *Diplopsalis* spp., and may also include other round brown cysts with problematic morphology such as *Diplopelta* sp. and *Diplopsalopsis* sp. and others described in Mertens et al. (2020).

For the same reason, *Echinidinium delicatum* and *E. granulatum*, both characterized by having hollow processes (Zonneveld and Pospelova, 2015), were grouped in *E. delicatum/granulatum*. On the other hand, taxa that could be misidentified during routine counts were included in the same group, namely cyst types for which

TABLE 2 | List of all dinoflagellate cyst taxa identified in this study and their corresponding biological (motile cell) names.

Autotrophic taxa		Heterotrophic taxa			
Paleontological name	**Biological name**	**Paleontological name**	**Biological name**	**Paleontological name**	**Biological name**
Alex-type (cf. calcareous cysts without ornamentation)	Unknown	Cysts of *Archaeperidinium minutum*	*Archaeperidinium minutum*	*Selenopemphix nephroides*	*Protoperidinium subinerme*
Cysts of cf. *Ensiculifera tyrrhenica* (*sensu* Li et al., 2020)	Cf. *Ensiculifera tyrrhenica*	*Brigantedinium* sp.	*Protoperidinium* sp.	*Selenopemphix quanta*	*Protoperidinium conicum*
Cysts of *Gymnodinium catenatum*	*Gymnodinium catenatum*	*Brigantedinium cariacoense*	*Protoperidinium avellana*	*Trinovantedinium applanatum*	*Protoperidinium shanghaiense*
Cysts of *Gymnodinium nolleri/microreticulatum* (30–40 μm diameter, according to Amorim et al., 2002)	*Gymnodinium* sp.	*Brigantedinium simplex*	*Protoperidinium conicoides*	*Votadinium calvum*	*Protoperidinium oblongum*-complex var. *latidorsale*
Cysts of *G. microreticulatum* (<30 μm diameter)	*Gymnodinium microreticulatum*	*Dubridinium caperatum*	*Preperidinium meunieri*	*Votadinium rhomboideum*	*Protoperidinium quadrioblongum*
Impagidinium aculeatum	Probably *Gonyaulax* sp.	*Dubridinium* sp.	Diplopsalid group	*Votadinium* sp.	*Protoperidinium* sp.
Impagidinium paradoxum	Probably *Gonyaulax* sp.	cf. *Diplopsalis*-type	Diplopsalid group	*Xandarodinium xanthum*	*Protoperidinium divaricatum*
Impagidinium sp.	Probably *Gonyaulax* sp.	*Echinidinium aculeatum*	Unknown (probably Protoperidinoid group)	Unidentifiable (brown) peridinoid cysts	Probably *Protoperidinium* sp.
Lingulodinium machaerophorum	*Lingulodinium polyedra*	*Echinidinium granulatum/delicatum*	Unknown (probably Protoperidinoid group)	Unidentifiable RBC (round brown cysts)	Protoperidinoid?
Operculodinium centrocarpum	*Protoceratium reticulatum*	*Echinidinium transparantum*	Unknown (probably Protoperidinoid group)	Unidentifiable SBC (spinny brown cysts)	*Protoperidinoid?*
Tuberculodinium vancampoae	*Pyrophacus steinii*	*Lejeunecysta oliva* (*sensu* Van Nieuwenhove et al., 2020)	*Protoperidinium* sp.		
Cysts of *Scrippsiella* cf. *trochoidea*	*Scrippsiella* cf. *trochoidea*	*Lejeunecysta* cf. *sabrina* (*sensu* Van Nieuwenhove et al., 2020)	Probably various species of *Protoperidinium* sp.		
Sphaerical-type (*sensu* Wall and Dale, 1968) (unknown calcareus cysts)	Unknown	*Lejeunecysta/ Quinquecuspis* (cingulum not visible)	Probably various species of *Protoperidinium* sp.		
Spiniferites bentorii	*Gonyaulax digitale* group	Cysts of *Polykrikos kofoidii* (*sensu* Matsuoka et al., 2009)	*Polykrikos kofoidii*		
Spiniferites delicatus	*Gonyaulax* sp.	Cysts of *Polykrikos schwartzii* (*sensu* Matsuoka et al., 2009)	*Polykrikos schwartzii*		
Spiniferites membranaceus	*Gonyaulax membranacea*	Cysts of cf. *Protoperidinium monospinum*	*Protoperidinium monospinum*		
Spiniferites mirabilis/hyperacanthus	*Gonyaulax spinifera* group	Cysts of *Protoperidinium americanum*	*Protoperidinium americanum*		
Spiniferites sp.	*Gonyaulax* sp.	Cysts of *Protoperidinium stellatum*	*Protoperidinium stellatum*		
Cysts of cf. *Thoracosphaera* sp.	cf. *Thoracosphaera* sp.	*Quinquecuspis concreta*	Probably *Protoperidinium leonis*		

the archeopyle or paracingulum were not visible and that presented a high degree of morphological variation, for instance, *Lejeunecysta/Quinquecuspis*, which includes dorsoventrally compressed brown cysts with peridinoid outline and pentagonal shape that may correspond to *L. sabrina*, *L. oliva* or *Q. concreta* (Images 6 to 8, **Supplementary Plate II**) (Van Nieuwenhove et al., 2020). Other peridinoid brown cysts without such pentagonal shape, with clear archeopyle involving the apical section and not classified as *Votadinium calvum* (Image 10, **Supplementary Plate II**) or *Votadinium*

rhomboideum (Gurdebeke et al., 2019) were classified as *Votadinium* sp. Moreover, *Brigantedinium* spp. includes cysts of *Brigantedinium* sp. with hidden archeopyle, and also some cysts of *Protoperidinium avellana* (*B. cariacoense*; Image 4, **Supplementary Plate II**) and *P. conicoides* (*B. simplex*). Finally, *Spiniferites* spp. includes unidentifiable species (*Spiniferites* sp.) and other species that were identified in some samples (e.g., *S. delicatus* and *S. bentori*) but could be misidentified in others due to their difficult orientation.

Environmental Data and Statistical Analyses

Samples were arranged in a hierarchical cluster constrained by latitude, using Bray-Curtis dissimilarity distances and CONISS method. On the other hand, Redundant Discriminant Analysis (RDA) was performed to explore the relationships between dinoflagellate cyst distributions and environmental gradients. Before RDA, Detrended Correspondence Analysis (DCA) was used to determine the behavior of taxa along the main environmental gradients. RDA was the method of choice for constrained ordination since the length of the first gradient is 1.84 SD, indicating mostly linear taxa responses (ter Braak and Prentice, 1988). All statistics were performed using R software v. 3.0.2. (R Development Core Team, 2013).

Because of their presumably similar ecological affinities, for clustering and RDA analyses, the round brown cysts *Brigantedinium* spp., *Diplopsalis*-type, *Dubridinium* spp., and unidentifiable round (smooth) brown cysts (which include broken or folded brownish cysts with round outline that probably correspond to one of the previous genera) – were grouped in RBC. Additionally, unidentified cysts were excluded and those groups for which identification was doubtful in some samples were grouped to the genus level. A total of 23 cyst types and square-root transformed percentage data (%) were used for RDA analyses (taxa that never contributed >1% were excluded). Note that very consistent results were obtained with or without data transformation.

Six variables were investigated in this study, namely: water depth (WD), sediment mean diameter (Gran), bottom temperature (BTT), sea-surface salinity (SSS), satellite-derived sea-surface temperature (SST), and sea-surface chlorophyll-a concentration (CHL). Initially, six parameters for each variable (except for WD and Gran) were explored by RDA to check their influence on the ordination of samples, namely: the global average, the global median value (50th percentile or p50), the value for the month with the lowest mean value, the value for the month with the highest mean value, and the averages of the trimester with the highest and lowest mean values. These parameters were calculated from daily values from 2003 to 2019; except for BTT and SSS, which were calculated from a data series corresponding to the period 2018–2020. These time intervals were selected as they correspond to the highest resolution of environmental data to which access was available. In the final RDA diagrams (**Table 1**), only the parameters with the highest weight in the ordination of samples were included. Our choices were based on statistical scores R^2, the variance explained and the *p*-value from random permutation tests (999 permutations at a significance level of $P \leq 0.05$). Additionally, redundant variables that strongly correlated with more significant variables were discarded (see Oksanen et al., 2015).

Oceanographic variables were obtained from satellite remote sensing and hydrodynamic numerical models. The daily numerical model solutions for bottom temperatures (BTT) and sea-surface salinities (SSS) were gathered from the E.U. Copernicus Marine Monitoring Service (CMEMS), namely from the Operational IBI (Iberian Biscay Irish) Ocean Analysis and Forecasting system, which is based on a (eddy-resolving) NEMO model application run at 1/36° horizontal resolution (Sotillo et al., 2015). The two satellite-derived variables, available as daily, 1 km resolution maps, were the sea-surface temperature (SST), from the Multi-scale Ultra-high Resolution (MUR) SST analysis (JPL, 2015; Chin et al., 2017), and chlorophyll-a (CHL) from CMEMS based on the Copernicus-GlobColour processor, namely from the North Atlantic Chlorophyll product (OCEANCOLOUR_ATL_CHL_L4_REP_OBSERVATIONS_009_098).

RESULTS

Estimation of Sediment Accumulation Rates

No box-corers were collected during the cruise, so establishing accurate sedimentation rates for sediment samples investigated in this study was not possible. However, in nearby areas (north of the Douro mud patch), Jouanneau et al. (2002) performed Pb analyses in 31 box-core samples collected at depths ranging from −39 to −213 m, and found that accumulation rates ranged between 0.05–0.40 cm $year^{-1}$. Considering the results by Jouanneau et al. (2002), we estimated that the top 1 cm of surface sediment samples collected off Aveiro-Figueira da Foz recorded between 2.5 and 20 years of cyst deposition. Moreover, the top 20 cm of surface sediment samples used for grain-size analyses would represent <400 years of deposition. We believe that this temporal mismatch between the two type of samples is not a major problem since the obtained grain-size distribution accurately represents the main (modern) distribution patterns observed in the study area, being consistent with available sediment cartography, such as the Seabed Substrate maps from EMODnet Geology (available at[1]) and the sedimentological charts from the Hydrographic Institute of Portugal[2],used as base to compile the EMODnet information. Therefore, we considered that the obtained grain-size distribution was well representative of modern sediment distribution and represents the best available data to be compared with the modern distribution of dinoflagellate cyst assemblages.

Grain Size and Dinoflagellate Cyst Distribution

Mean grain diameter ranged from 0.06 to 2.20 mm. Sands dominated all samples with percentages varying between 51

[1]https://www.emodnet-geology.eu/map-viewer/?p=seabed_substrate

[2]https://www.hidrografico.pt/op/40

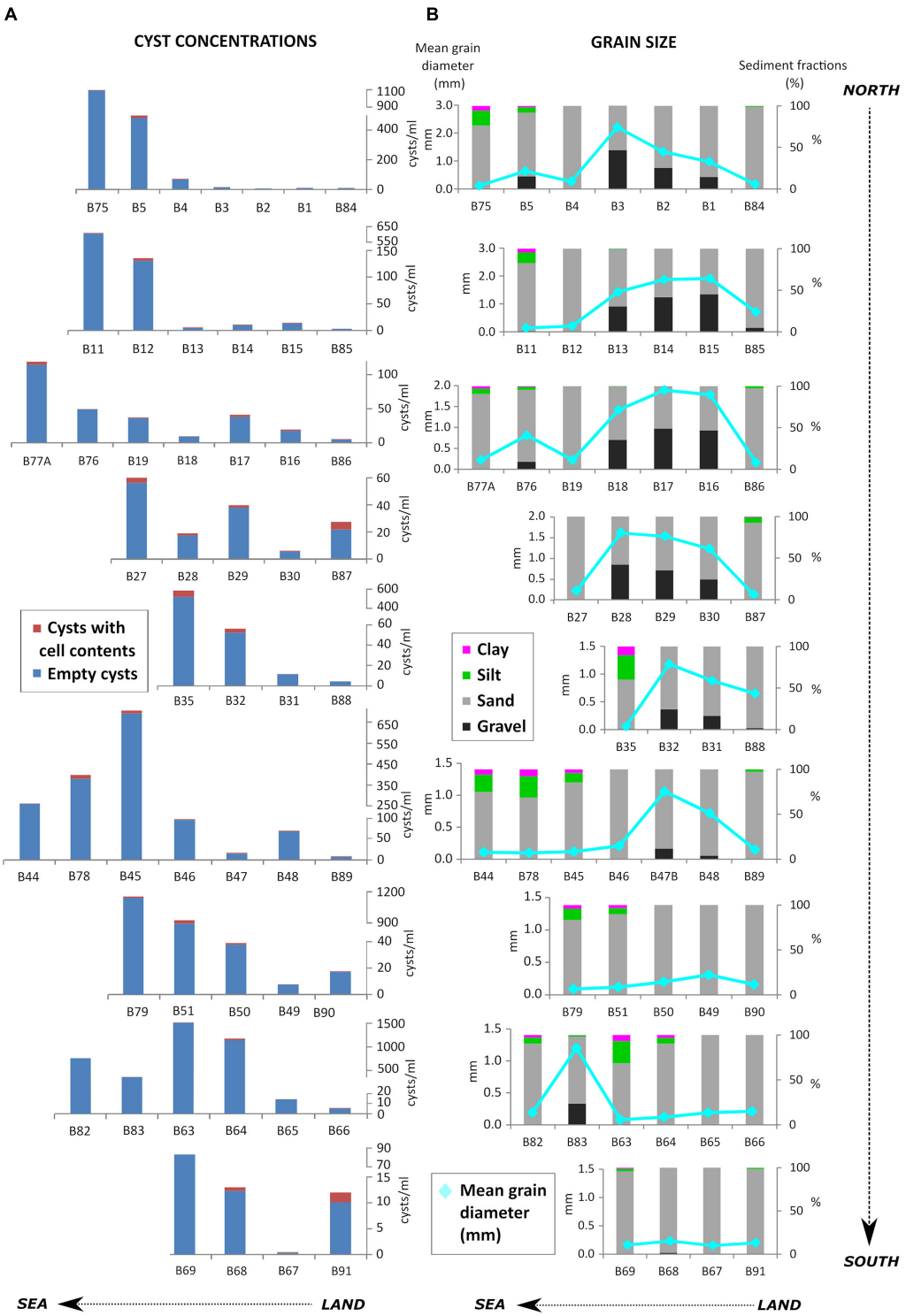

FIGURE 2 | Spatial distribution of cysts (empty cysts and cysts with cell contents) (cysts·ml^{-1}) **(A)** and sediment grain size **(B)** along the nine transects studied.

and 100% (**Supplementary Table 3**). Coarsest samples usually corresponded with stations at mid-depths. Grain size also increased in northern transects, in front of Ria de Aveiro, with gravel percentage ranging 40–49% in samples B3, B14, B15, B16, B17, and B28. In contrast, proportions of finer sediments (silt and clay) increased southwards and in deeper samples (**Figure 2B**).

Cyst concentrations ranged between 0.5 and 1478.4 cysts·ml^{-1}. The lowest concentrations were observed in

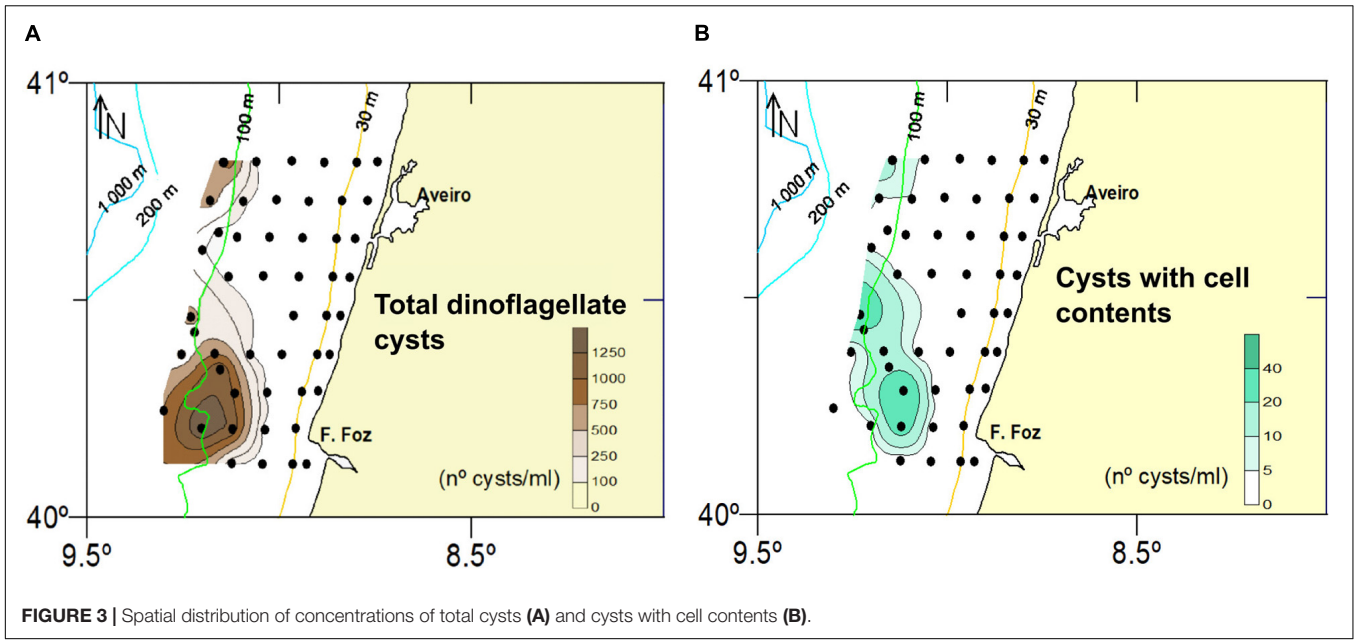

FIGURE 3 | Spatial distribution of concentrations of total cysts **(A)** and cysts with cell contents **(B)**.

coarse samples close to the coast, whereas the highest values were generally found in deeper stations with finer sediments (>500 cyst·sml^{-1} in stations B63, B64, B82, B51, B79, B45, B35, B11, B75) protected in general by rock outcrops (**Figures 1**, **2A,B**, and **3A**).

A total of 45 dinoflagellate cyst types were identified, excluding unidentifiable types round brown cysts (RBC), spiny brown cysts (SBC), and brown peridinoids (**Table 2**). Morphotype richness or number of cyst types per sample is shown in **Supplementary Table 4** (Unidentifiable types are counted as one type), with a maximum of 33 and a minimum of 10 cyst types. Morphotype richness generally increased northwards and at mid depths.

Empty cysts dominated all cyst assemblages (**Figure 2A**). Full cysts were observed in 22 cyst types: *Alexandrium*-type, *Brigantedinium* spp., *Dubridinium caperatum, G. catenatum*, *G. nolleri/microreticulatum*, cf. *Lejeunecysta sabrina, P. reticulatum*, *Protoperidinium americanum*, *P. conicum, P. shanghaiense*, *P. subinerme, Spiniferites* sp., *S. membranaceus*, *S. mirabilis/hyperacanthus*, *Votadinium* sp., and *V. rhomboideum*, as well as some unidentifiable RBC, SBC and brown peridinoids. Concentrations of full cysts (as well as total cysts) increased southwards and offshore, i.e., 100 m isobath (**Figures 3A,B**), while proportions tended to increase in shallower samples (**Figure 2A**). However, counts of full cysts were generally very low (0–56), therefore, the observed trend in their proportions may not be significant.

Full cysts of the HAB species *G. catenatum* and *P. reticulatum* occurred in negligible amounts while no full cysts of *L. polyedra* were recorded. In contrast, many full cysts of calcareous taxa (*Scrippsiella trochoidea*, spherical-type cf. *Scrippsiella* sp., cf. *Ensiculifera tyrrhenica*) and RBC were identified (**Supplementary Table 4**).

The cysts of cf. *E. tyrrhenica* have a calcareous wall, yellowish under bright field microscopy. It is characterized by a flat side with pentagonal outline and a triangular side suggesting a "Napoleon hat" (Montresor et al., 1993) (Images 2 and 4, **Supplementary Plate I**). Cysts are 30–37 μm in diameter and the cyst content has a clear red accumulation body (Images 1–4, **Supplementary Plate I**). These morphological features coincide with those described for cysts of *Pentapharsodinium tyrrhenicum* (Balech) Montresor, Zingone & D.Marino ex Head, described in Montresor et al. (1993), which has been recently transferred to the genus *Ensiculifera* (Li et al., 2020). To date, on the Atlantic Iberian margin, *E. tyrrhenica* has only been reported in this study and in Amorim (2001). In the latter study, a dinocyst survey was done along the whole Portuguese coast but *E. tyrrhenica* was only recorded in Ria de Aveiro, located in the vicinity of the present study area.

Regarding trophic affinities, proportions of heterotrophic species generally increased northwards, the exception being samples B75 and B11 where proportions of autotrophic cysts were higher than 50%. They also showed a land-sea gradient increasing (>50%) in shallower stations close to the coast (**Figures 4**, **5**), *Brigantedinium* spp. (mean proportion of 11.7%), RBC (10.1%) and *Lejeunecysta/Quinquecuspis* (4.55%) being the most abundant heterotrophic cyst types (**Figure 6**). In contrast, proportions of autotrophic species increased southwards and in deeper samples (**Figures 4**, **5**), *G. catenatum*, *P. reticulatum*, *S. mirabilis/hyperachantus* and *L. polyedra* being the most abundant autotrophic cyst types, with mean proportions (full + empty cysts) of 16.2, 8.4, 5.7, and 4.9%, respectively (**Figure 6**). *Gymnodinium catenatum* was always a relevant component of the cyst assemblage and showed distribution centers close to the 100 m isobath (**Figure 7**).

The highest proportions of autotrophic cysts (38.2–78.4%) were recorded in the B82-B66 transect, located in front of

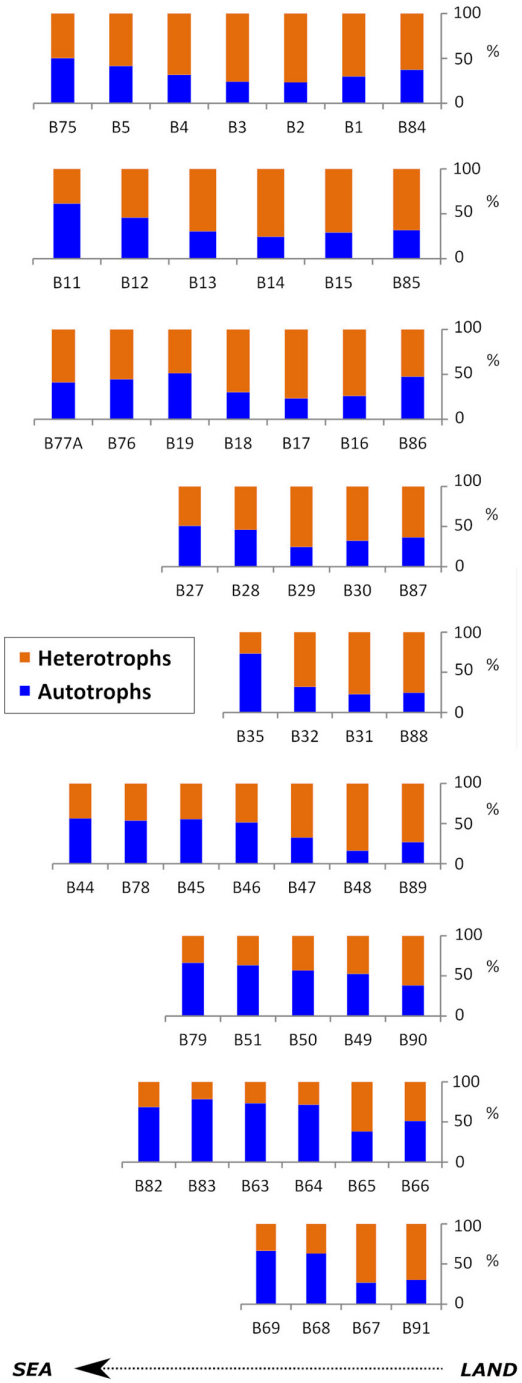

FIGURE 4 | Spatial trends in relative abundances (%) of heterotrophic (orange) and autotrophic (blue) taxa along the nine land-sea transects studied.

Mondego cape (**Figures 1B**, **4**). These samples also recorded particularly high relative abundance values of the potentially toxic species *P. reticulatum* (9–36%) and *L. polyedra* (1.4–18.4%) (**Figure 7**). Although close to the 100 m isobath, their distribution centers were displaced south in relation to the distribution center of *G. catenatum* (**Figure 7**).

Multivariate Analyses and Environmental Influences

According to cluster analysis constrained by latitude, cyst assemblages could be classified in three groups (southern, intermediate and northern samples). Clustering also indicated that the major change in cyst composition was between northern and the remaining (southern + intermediate) samples, cyst assemblages from southern and intermediate samples being more similar (**Figures 8A,B**, **9A,B**).

Redundant discriminant analysis (RDA) helped in investigating the main environmental factors influencing dinoflagellate cyst distribution. The final RDA model (**Figures 9A,B**) significantly ordinated the samples according to cyst composition and the influence of environmental variables (p-value < 0.05). The variance explained by the two main axes (RDA1 e RDA2) was 30.4%. Mean sea-surface temperature (SST) of the warmest trimester (July to September) and water depth (WD) were the most relevant environmental variables (i.e., those contributing the most to explain the variability of cyst assemblage distribution), followed by grain size (Gran) and chlorophyll-a concentration (CHL). Despite the small amplitude of variation of the SST values used for the RDA (see SD, **Table 1**), it represents an average of daily values for a period of 16 years (2003 to 2019), and therefore, small changes in SST could actually represent relevant changes in the environment.

The main variability gradient was defined by RDA1 (explaining 25.1% of the total variance), which was positively correlated with SST, SSS and WD and negatively correlated with CHL, BTT and Gran. It also reflected relevant differences between northern samples (generally negative RDA1 values), and southern/intermediate samples (generally positive values on RDA1), in good agreement with the cluster classification results (**Figure 8**). Northern samples positively correlated with CHL, BTT and Gran, whereas southern samples positively correlated with SST, SSS and WD (**Figure 9A**).

Heterotrophic cyst taxa ordinated to the left side of the biplot, with CHL, BTT and Gran. The cyst taxa with the most negative scores on RDA1 were *Q. concreta* and RBC (**Figure 9B**). In contrast, autotrophic taxa generally presented positive values on RDA1, with SST, SSS and WD. *G. catenatum* and *P. reticulatum* had the highest values on RDA1. *G. catenatum*, *G. microreticulatum,* and *Scripsiella* sp., plotted on the upper right quadrant with WD. In contrast, *P. reticulatum*, *L. polyedra, S. mirabilis/hyperacanthus,* and *Spiniferites* sp. plotted on the lower right quadrant, representing warmer conditions (**Figure 9B**). The distribution of the heterotrophic species *P. americanum* did not follow the general pattern detected for other heterotrophic species. *P. americanum* ordinated to the right, with most of the autotrophic species.

An inshore-offshore environmental gradient was also reflected in RDA. Deeper samples were ordinated to the upper right quadrant of the biplot (**Figure 9A**), with higher abundances of *G. catenatum* (**Figure 9B**). On the other hand, shallower samples

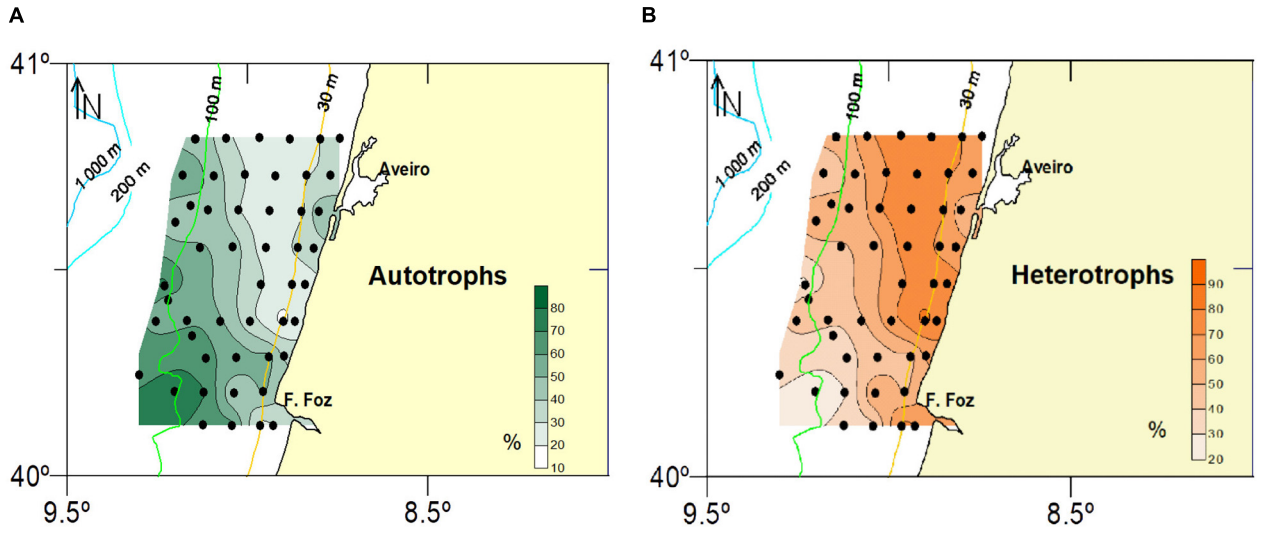

FIGURE 5 | Spatial distribution of relative abundances (%) of autotrophic **(A)** and heterotrophic **(B)** cyst taxa.

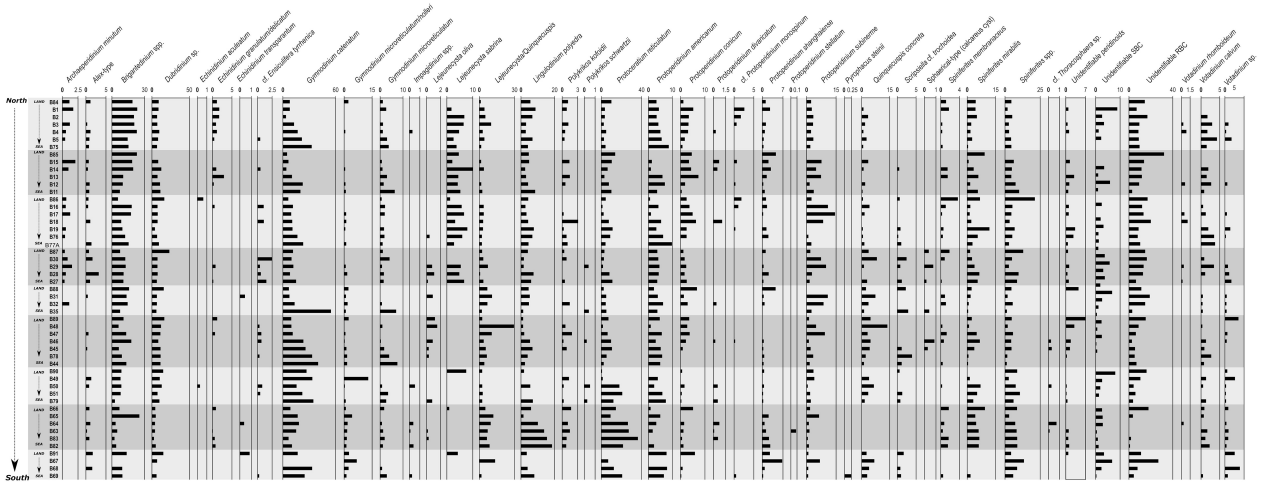

FIGURE 6 | Dinoflagellate cyst percentages obtained for the studied 51 surface samples. Samples are arranged by nine transects perpendicular to the coast, from north to south (top to bottom). Those cyst types for which identification was doubtful were summed to a higher category, i.e., *Brigantedinium* spp. includes *Brigantedinium* sp. and cysts of *Protoperidinium avellana* and *P. cariacoense*; *Dubridinium* spp. includes *Dubridinium* sp. and *D. caperatum*; *Impagidinium* spp. includes *Impagidinium* sp., *I. paradoxum*, and *I. aculeatum*; *Spiniferites* spp. includes *Spiniferites* sp., *S. bentorii*, and *S. delicatus*; RBC includes unidentifiable round browns and cf. *Diplopsalis*-type.

ordinated to the lower left quadrant of the biplot (**Figure 9A**), with higher proportions of *Protoperidinium* species and most of heterotrophs (**Figure 9B**).

DISCUSSION

This study investigated the distribution of benthic dinoflagellate resting cysts in recent sediments from the shelf off Aveiro-Figueira da Foz (Atlantic Iberian margin) in relation with present day environmental drivers. These studies are particularly relevant since cysts are the only fossilizable stage of dinoflagellates and understanding how they reflect present day environmental conditions will contribute to a better interpretation of environmental signals from stratigraphic cyst records.

Distribution of Sediments and Cyst Concentrations

Coastal hydrodynamics and topography play an important role in the distribution of sediments and dinoflagellate cysts. The main topographic and morphological features in the shelf area covered by this study that may affect the distribution patterns of sediments and dinoflagellate cysts are the Cape Mondego and sheltered rocky outcrops (**Figure 1B**). Coarse sediments are common in the shelf of the Iberian Atlantic coast, while

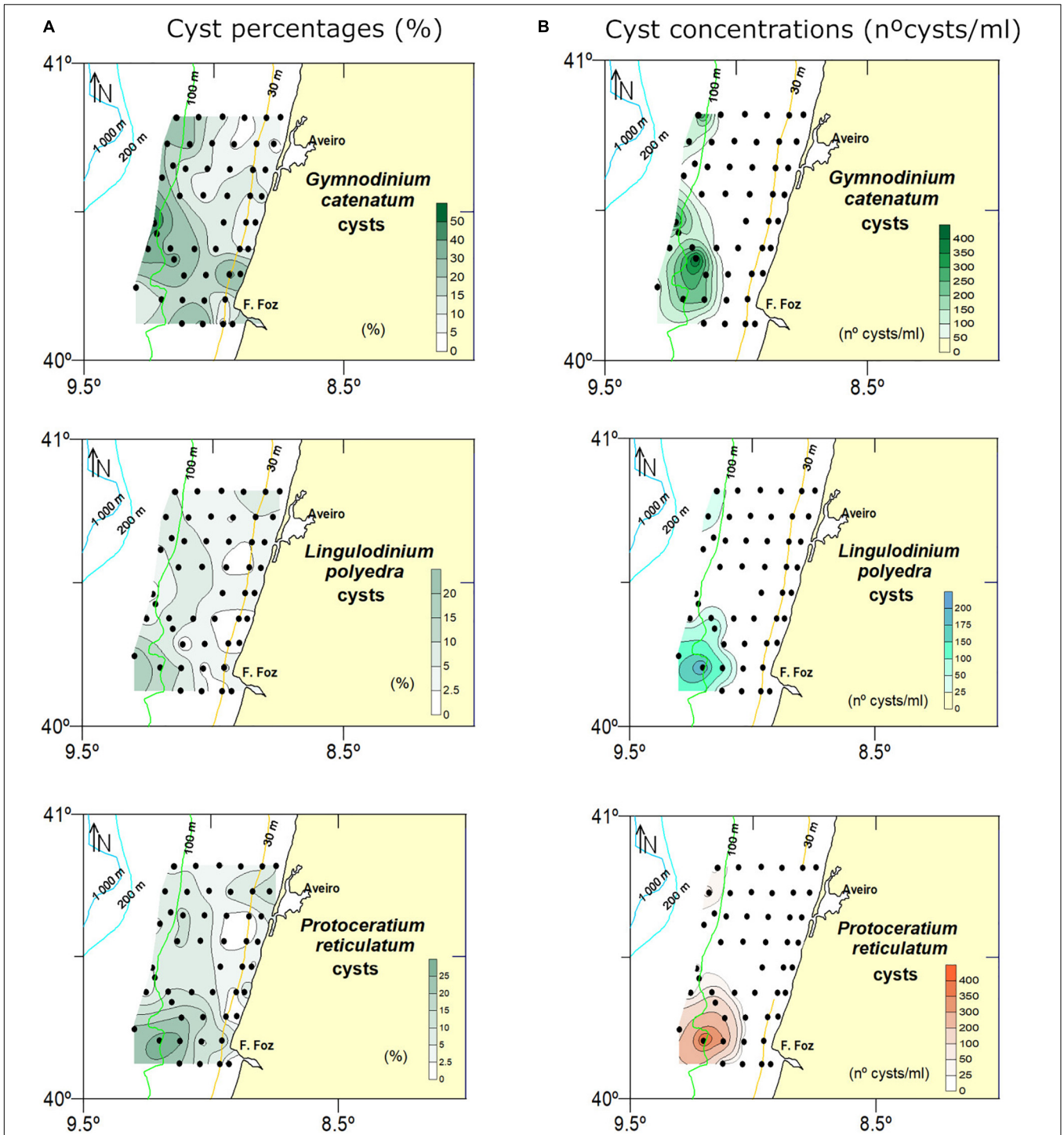

FIGURE 7 | Spatial trends in relative abundances **(A)** and concentrations **(B)** of cysts of the three HAB species (*Gymnodinium catenatum, Lingulodinium polyedra, and Protoceratium reticulatum*).

sheltered deposits of mud (silt and clay) are strongly influenced by the vicinity of rocky outcrops that act as traps favoring the accumulation of fine sediments (**Figure 1B**; Dias et al., 2002; Oliveira et al., 2007). Additionally, in coastal areas, sediments can be resuspended by waves and tidal currents and while sands are deposited rapidly once conditions calm down, finer sediments (cysts included) are more susceptible to be transported offshore (Oliveira et al., 2002). This could partially explain the decrease in sediment grain size with water depth observed in the study area (**Figure 2B**).

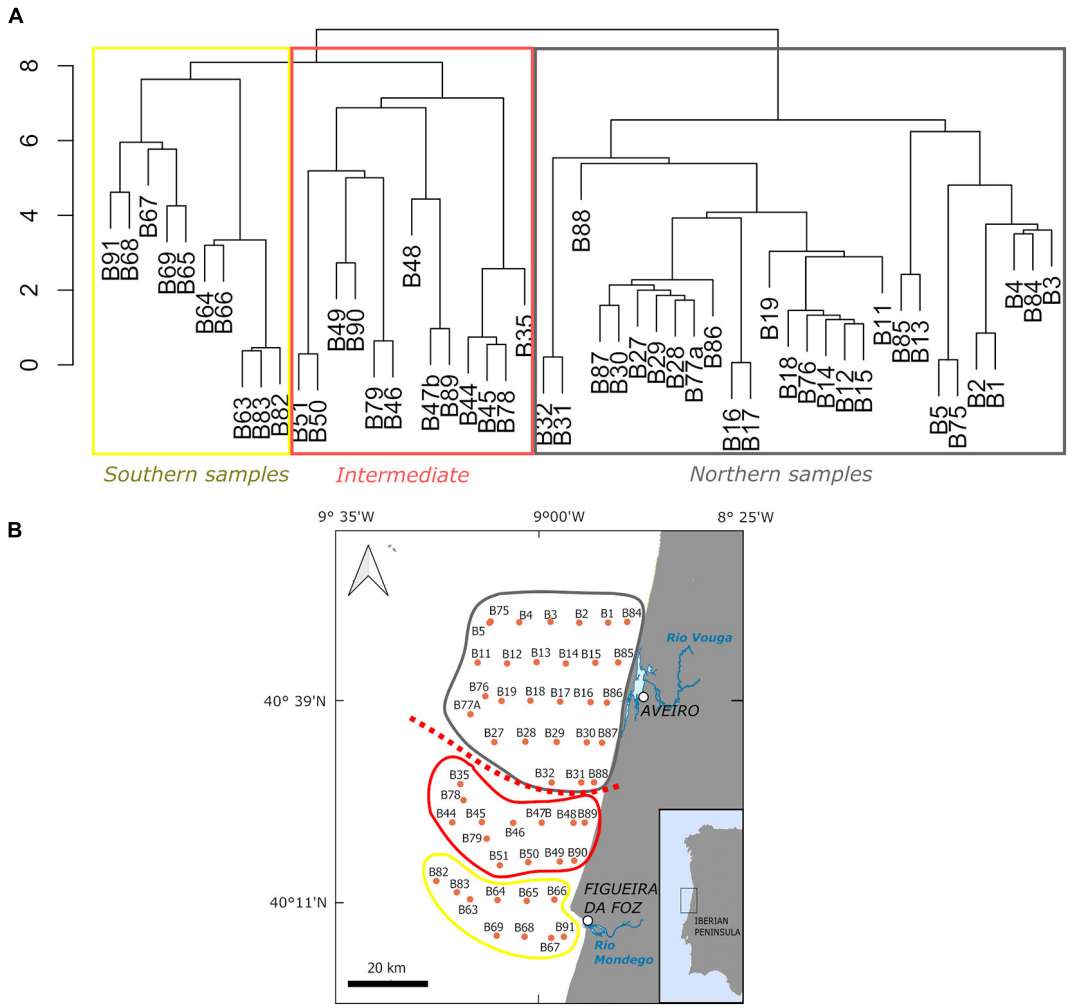

FIGURE 8 | Classification results from cluster analysis (constrained by latitude) performed on untransformed percentage data using Bray Curtis dissimilarity distances and Coniss method **(A)**. The dashed red line in the map **(B)** separates the main two groups of samples according to the highest differences in their cyst assemblages.

Changes in total cyst concentrations along the 9 transects perpendicular to the coast (**Figure 2A**) were also highly related to sediment grain size. Both cyst concentrations and fine-grained sediments (silt and clay) increased seawards and southwards (**Figures 2A,B**, **3A**). This relationship, recognized since early works on dinoflagellate cyst assemblages from recent sediments, supports the interpretation of cysts behaving as fine silt particles in the sedimentary regime (Dale, 1976).

Environmental Influences on the Dinoflagellate Cyst Assemblages

The dinoflagellate cyst assemblages (concentrations and relative abundances) revealed marked inshore-offshore and latitudinal gradients that may reflect different environmental factors. It should be noted that shelf surface sediments are the result of several years of deposition, reworking and bioturbation. Likewise, the associated dinoflagellate cyst assemblages represent an integration in time and space of the species encystment dynamics and of sedimentation processes. They reflect the dominant ecological processes over several years rather than a seasonal signature (Dale, 1976).

Along the W Iberian shelf, the oceanographic process regarded as the major source of seasonal and spatial phytoplankton variability is coastal upwelling, which usually lasts from spring to early autumn, with a peak in July (Moita, 2001; Pitcher et al., 2010). Phytoplankton succession is characterized by a strong link to the mixing-stratification patterns both at the seasonal and the upwelling event scale. In general, spring and summer upwelling events are characterized by the dominance of chain-forming diatoms, and the summer-autumn stratified conditions by dinoflagellates. In some years, the autumn upwelling-downwelling transition, as well as summer upwelling relaxation, are dominated by chain forming dinoflagellates such as the HAB species *G. catenatum* (Moita et al., 1998; Pitcher et al., 2010).

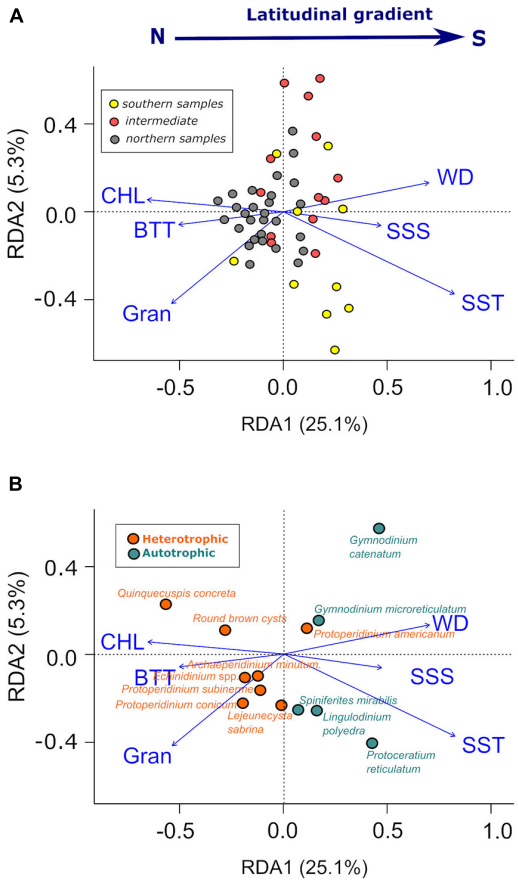

FIGURE 9 | Ordination of samples and environmental parameters **(A)**, and cyst taxa and environmental parameters **(B)**. The three groups defined by cluster are represented by different colors **(A)**. Only the most significant cyst types (those with the highest RDA1 and RDA2 values) are represented **(B)**.

In this study, Redundant discriminant analysis (RDA) helped to explore the relationships between environmental parameters – grain-size (Gran), water depth (WD), sea-surface temperatures (SST), sea-surface salinities (SSS), bottom temperatures (BTT) and chlorophyll-a concentration (CHL) (**Table 1**) – and the dinoflagellate cyst assemblages in surface samples (**Figures 9A,B**). It should be noted that the spatial resolution of the environmental data is a bit lower than the dinoflagellate cyst records. Despite this, the available SST data seems to well represent the main environmental distribution gradients that predominated in the study area for the last decades (Peliz et al., 2002; Oliveira et al., 2019).

Redundant Discriminant Analysis suggests the existence of two main environmental regimes (**Figures 9A,B**). One (positive values on RDA1), which included the southern and offshore (deeper) sites, was characterized by higher SST, lower BTT and lower primary productivity (lower CHL), suggesting warm stratified conditions. The other (negative values on RDA1), which included the northern sector and inshore (shallower) sites, was characterized by lower SST, higher BTT and enhanced primary productivity (higher CHL), suggesting upwelling influence.

These two main environmental regimes were reflected on the cyst assemblages by a clear trophic segregation. In the first case, autotrophic taxa, such as *P. reticulatum*, *L. polyedra*, *S. mirabilis/hyperacanthus*, *G. catenatum,* and *G. microreticulatum*, dominated the assemblage, while in the second case heterotrophs were the dominant group, particularly RBC, including *Brigantedinium* spp., and *Q. concreta* (**Figure 9B**).

Heterotroph dominance has been previously identified as the primary cyst signal for upwelling (Dale, 1996; Dale et al., 2002; Dale and Dale, 2002; Bringué et al., 2014). This interpretation has been supported by a 2-year sediment trap study in Santa Barbara Basin, North-East Pacific, influenced by seasonal upwelling (Bringué et al., 2013). The study covered several cycles of upwelling and relaxation and indicated that active upwelling was characterized by an increase in the fluxes of *Brigantedinium* spp. (*Protoperidinium* spp.) and other heterotrophic species such as cysts of *Protoperidinium conicum*. The authors also reported that biogenic silica, used as a proxy for diatom production, showed a strong positive and significant correlation with heterotrophic cyst types, suggesting a causal predator-prey relationship between the two groups. Very little is known on the effect of turbulence in heterotrophic dinoflagellates. Smayda (2002) reviewed the importance of swimming speed in the capacity of dinoflagellates to overcome vertical and horizontal velocity rates. Heterotrophs, namely protoperidinioids, were among the species that presented swimming speeds compatible with surviving upwelling velocity rates. This would allow them to prey on species characteristic of active upwelling, such as diatoms. Evidence from other studies investigating dinoflagellate cysts in relation to hydrological conditions and marine productivity also related the distribution of heterotrophic dinoflagellate cysts to the distribution of their prey, especially diatoms (e.g., Price and Pospelova, 2011; Elshanawany and Zonneveld, 2016). In the study area, the upwelling pattern is characterized by an onshore narrow band of cold water with the isotherms almost following the bottom contours (Fiúza, 1983; Relvas et al., 2007), with a zone of higher upwelling probability running parallel to the coast (**Figure 1C**). It is noteworthy that this pattern can also be seen in the distribution of heterotroph dominance (particularly RBC) in inshore samples and the northern sector (**Figure 5B**). In W Iberia, as in other upwelling areas, diatoms are the dominant group during active upwelling when vertical stratification is weakened (Moita, 2001; Moita et al., 2003; Pitcher et al., 2010; Villamaña et al., 2017) suggesting the observed distribution of heterotrophic dinoflagellates is reflecting the abundance of their prey as observed in similar systems. These results are consistent with the use of the "heterotroph signal" as an upwelling productivity signal in W Iberia (Dale, 1996).

The interpretation of the heterotroph dominance as an upwelling signal is preferred to other nutrient enrichment processes, such as nutrient loads from river input, since this would also promote increased stratification which would favor autotrophic dinoflagellates relative to other non-flagellated groups such as diatoms. The latitudinal gradient on heterotrophic dominance (higher abundance in northern sites) can at least partially be explained by a recurrent upwelling front observed

on the shelf north of the study site, offshore the Douro estuary (e.g., Haynes et al., 1993; Cordeiro et al., 2015), and the coincidence with a zone of higher upwelling probability (**Figure 1C**; Relvas et al., 2007), i.e., the greater abundances of heterotrophic cysts in northern samples responding to increased productivity (**Figure 9B**).

The southern and offshore sites, characterized by warm stratified conditions (positive side of RDA1), were dominated by autotrophic cyst taxa (**Figures 9A,B**). However, the statistical analysis suggested two groups that may represent distinct ecological signals. One group, characterized by *P. reticulatum*, *L. polyedra* and *S. mirabilis/hyperacanthus*, and a second group characterized by *G. catenatum, G. microreticulatum* and the heterotrophic species *P. americanum*.

The first group showed a strong (positive) correlation with SST (**Figure 9B**). *Spiniferites mirabilis* has a wide geographical distribution in temperate to equatorial regions and occurs in all major upwelling areas (Zonneveld et al., 2013). In the Northeastern Pacific, influenced by upwelling, Pospelova et al. (2008) described *S. mirabilis* associated with a warm water assemblage which also included *L. polyedra*. In the Po river estuary (Eastern Mediterranean), Zonneveld et al. (2009) also found an association between *S. mirabilis* and warm upper waters. Regarding *L. polyedra*, globally, modern distribution of cysts has been related to coastal environments of low and middle latitudes, with a distribution center south of the Iberian Peninsula, in the Gulf of Cadiz, and the northwest African coast (Lewis and Hallett, 1997; Marret et al., 2020; de Vernal et al., 2020). At regional scales, many studies related high abundances of this cyst to warm and stratified environments (e.g., Leroy et al., 2013; Ribeiro et al., 2016). The flagellate stage of *L. polyedra* is known to perform daily vertical migrations (Lewis and Hallett, 1997 for a review) which may represent an important competitive advantage in stratified environments. Along the S and W Iberian shelf, planktonic blooms of *L. polyedra* have been reported in late summer-early autumn associated with warm stratified waters (SST of ∼17°C) that were adjoined by upwelling plumes (Amorim et al., 2001, 2004). In agreement with these observations, results from the above-mentioned sediment trap study by Bringué et al. (2013) in the seasonal upwelling system off Southern California, showed that higher fluxes of theca and cysts of *L. polyedra* coincided with periods of higher SST, stronger stratification and reduced primary productivity. It was even suggested that 15°C could represent a lower temperature threshold for increased *L. polyedra* fluxes. These observations support the interpretation that in seasonal upwelling systems, as suggested herein, the increased abundance of *L. polyedra* is the main signal for an increase in SST and water stratification. This is in good agreement with previous reports of cysts of *L. polyedra* (=*Lingulodinium machaerophorum*) from areas adjoining upwelling systems off South California and Northwest Africa (Dale, 1996).

Protoceratium reticulatum (=*Operculodinium centrocarpum*) is considered one of the most cosmopolitan species (Wall et al., 1977; Dale, 1996; Marret et al., 2020; de Vernal et al., 2020). Recent work has shown the existence of at least three genotypes with different ecological preferences (Wang et al., 2019). Despite this, cysts of *P. reticulatum* have been successfully used as part of ecological signals related with environmental instability in different marine ecosystems. This is the case for the coastal/oceanic transition, frontal zones or the instability associated with the propagation of river plumes (Dale, 1996; Dale et al., 2002). Studies on the fossil and sub-fossil record of dinoflagellate cysts in the NW Iberian shelf have found increased abundances of *P. reticulatum* associated with major environmental shifts (Amorim and Dale, 2006; Ribeiro et al., 2016; García-Moreiras et al., 2018, 2019).

Relvas et al. (2007) investigated the average effect of upwelling structures along the Portuguese coast and found a relatively weak upwelling signal and low frontal probability zone over the mid-shelf (between ∼100 and 200 m depth) of the present study area (**Figure 1C**), coincident with observations by Oliveira et al. (2019) of a cyclonic area limited inshore and offshore by upwelled waters (their Figure 10). The high relative abundance of *P. reticulatum* and the presence of *L. polyedra* in the outer stations of the southern transects is here interpreted as characterizing the location of the transitional zone between more active inshore upwelling and warmer offshore waters (compare **Figures 1C**, **7**). This would be in agreement with the concept of upwelling relaxation taxa proposed by Smayda and Reynolds (2001, 2003) for *L. polyedra* and *P. reticulatum*. The robustness of this signal could be further tested in the future extending the sampling area offshore well into the low frontal probability zone.

Ribeiro et al. (2016) investigated the main changes in cyst records in the NW Iberian shelf during the last ∼150 years. They reported a many fold increase in total cyst abundance that was concomitant with the increase in *L. polyedra* and *P. reticulatum*. This was interpreted as reflecting the combined effect of warming and increased water stability. In the Ria de Vigo, further north in the west Iberian margin (RdV, **Figure 1A**), García-Moreiras et al. (2018) also interpreted *L. polyedra* as an indicator of warm stratified environments, related to river inputs. Their interpretations are reinforced by a good correspondence between the highest abundances of this species in the dinoflagellate cyst record and a period of increased annual precipitations, as indicated by climate data directly measured and also inferred from independent proxies (tree ring reconstruction). Data presented in the present study based on recent cyst distributions (**Figures 7**, **9B**) supports these interpretations. Besides, they are in line with various studies worldwide (e.g., Amorim and Dale, 2006; Leroy et al., 2013; Ribeiro et al., 2016; García-Moreiras et al., 2018; de Vernal et al., 2020) that indicated a strong correlation between SST and *L. polyedra* abundances, supporting the utility of this cyst species as an indicator of warm and stratified environments.

The second group, characterized by high abundances of *G. catenatum*, the single species with the highest relative abundances in the study area, seems to reflect a different ecological niche from other autotrophs. It plotted the most positive on RDA1 with a strong association with deeper waters (**Figures 7**, **9B**). Latitudinally, it was particularly abundant (percentages) in the intermediate transects (i.e., red dots in **Figure 9A**).

The upwelling pattern in the study region is characterized by two upwelling frontal zones that tend to follow the depth contours: a narrow coastal band and further offshore close to the shelf break (Relvas et al., 2007), which coincides with the zones of high frontal probability represented in **Figure 1C**. The high relative abundances of *G. catenatum* in deeper samples following the 100 m isobath may be linked to these upwelling fronts. Indeed, Moita et al. (1998) reported high abundances of the vegetative stage at mid-shelf, related to the offshore displacement of blooms. More recent observations recorded the presence of *G. catenatum* in the inshore side of upwelling plumes where currents may be reduced and *G. catenatum* may develop close to the core of the upwelling plume without being advected away (Moita et al., 2003). This is consistent with the fact that coastal outbreaks of this species typically occur during the first late-summer/autumn downwelling events, when these offshore populations may be advected to the coast (e.g., Bravo et al., 2010; Díaz et al., 2019). High abundances of *G. catenatum* cysts may thus reflect the association of this species with upwelling fronts in W Iberia. Several authors have proposed the importance of chain formation as an adaptive strategy in upwelling areas (Fraga et al., 1988; Smayda and Reynolds, 2003). More recently, Smayda (2010) emphasized that although chain formation may be an advantage in turbulent waters associated with upwelling, chain-forming dinoflagellates are the exception and not the rule in upwelling systems and probably other factors such as temperature tolerance play an important role in species selection.

The previous interpretations of the distribution of dinoflagellate cyst assemblages in surface sediments and its comparison with present-day environmental data suggest that, in the study area, cysts are mainly reflecting the hydrographic conditions observed during the summer upwelling season. This season corresponds to the period of highest primary productivity (Moita, 2001). Interestingly, Abrantes and Moita (1999) investigated the planktonic communities of diatoms and coccolithophores along the Portuguese coast under winter (non-upwelling) and summer (upwelling) conditions and how they compared with the sediment record. Their results indicated that the sediment assemblages reflected mainly the water column distribution observed during the upwelling season.

Regarding the distribution of *P. americanum*, the weight in the ordination analysis is low and interpretations should be considered with caution. However, our results suggest that similarly to *G. catenatum* this species may prefer transitional waters between less productive and stratified environments (lower right quadrant, **Figure 9B**), and more productive environments associated to upwelling fronts (left side of RDA, **Figure 9B**). Existing studies on the distribution of this cyst and environmental gradients do not reflect a distinct distribution from other heterotrophs, indicating that its distribution is associated – but not restricted to – productive waters near upwelling cells (Dale, 1996; Marret and Zonneveld, 2003; Ribeiro and Amorim, 2008; Zonneveld et al., 2013). Zonneveld et al. (2013) also refer the preference for fully marine environments. Concordantly, the RDA indicates the distribution of *P. americanum* associated with more saline (and deeper) environments in the study area (**Figure 9B**), if compared to other heterotrophs.

Finally, a few considerations on the distribution of HAB species and the role of benthic cysts in HAB formation. In the present study, we recorded cysts of three dinoflagellate species that may be potentially toxic and produce Harmful Algal Blooms (HAB) in the Atlantic Iberian margin, namely *G. catenatum*, *L. polyedra* and *P. reticulatum*. Very high percentages of *G. catenatum* cysts (**Figure 7**) reflect a long history of blooms along the NW coast of Portugal. However, the almost absence of viable cysts in surface sediments is additional evidence supporting the hypothesis that this species does not rely on benthic cyst beds for seeding planktonic blooms (Fraga et al., 1993; Moita et al., 1998; Amorim et al., 2002; Bravo et al., 2010). Although blooms of *G. catenatum* have been studied in W Iberia for more than 40 years, it is still not fully understood which factors other than life cycle traits (physical or biological) may be involved in the initiation and successful development of blooms.

The yessotoxin producers *L. polyedra* and *P. reticulatum* reached high relative abundance in the southern transects (∼20 and 40% respectively). However, as for *G. catenatum*, the percentage of cysts with cell contents was very low suggesting that in the study area there is not a build-up of significant cyst beds of these two species. This interpretation is supported by a previous cyst survey along the coast of Portugal, where the main distribution center for *L. polyedra* cysts occurred in the south coast (Amorim et al., 2004). Regarding *P. reticulatum,* the absence of a good correspondence between reports of vegetative planktonic populations and the cyst record has been previously recognized (Dale, 1976). Several hypotheses were put forward which included the mismatch between phytoplankton studies and the occurrence of planktonic populations of *P. reticulatum*, and/or a species specific high cyst:motile cell ratio during the encystment process. So far, no harmful events have been associated with *P. reticulatum* in W Iberia. However, the high abundance of cysts in sediments prompts investigation on the ecology and toxicity of regional strains.

CONCLUSION

The study of the distribution of dinoflagellate cyst assemblages in 51 surface sediment samples off Aveiro-Figueira da Foz revealed marked land-sea and latitudinal gradients. Summer coastal upwelling was identified as the main ecological gradient driving dinoflagellate cyst assemblages in the study area.

Redundant analysis (RDA) on relative abundances revealed the existence of two main environmental regimes. One included the southern and offshore sites and was characterized by higher SST, lower BTT and lower primary productivity (lower CHL), suggesting warm, stratified and less productive environments. The other regime, which included the northern sector and inshore sites, was characterized by lower SST, higher BTT and enhanced primary productivity (CHL), suggesting the influence of upwelling.

Three main ecological signals were identified in the dinoflagellate cyst assemblages:

i) The heterotroph signal as the main upwelling signal;
ii) The dominance of *P. reticulatum* and *L. polyedra* signal, indicative of warm stratified conditions, possibly reflecting transitional environments between more active inshore upwelling and warmer offshore waters;
iii) The *G. catenatum* signal, the main signal for the presence of mid-shelf upwelling fronts.

The almost absence of viable cysts of the toxic and potentially toxic species *G. catenatum L. polyedra* and *P. reticulatum* in surface sediments, suggests that in the study area, for these three species, there is no build-up of significant cyst beds and thus planktonic populations must depend on other seeding processes.

These results are the first detailed distributions of modern dinoflagellate cysts in the NW Iberian Atlantic margin (off Portugal). Despite the uncertainties related to sediment and cyst transport, post-depositional processes and the possible disparity between the time scale of the cyst record and the time scale of the environmental data used, cyst distributions show a fairly compelling coincidence with hydrographic features during the summer upwelling season in the study area. This means that modern dinoflagellate cyst assemblages are reflecting water column characteristics and may be used as supporting evidence for the interpretation of stratigraphic cyst records and reconstruction of past marine ecosystems in W Iberia.

DATA AVAILABILITY STATEMENT

The original contributions presented in the study are included in the article/**Supplementary Material**, further inquiries can be directed to the corresponding author/s.

AUTHOR CONTRIBUTIONS

AA participated in the oceanographic campaign to obtain surface sediment samples and water depth data. AA, PO, and AO planned the research. Sediment texture analyses and statistics were performed by AO and AS. Oceanographic data collection and analysis was performed by PO. Dinoflagellate cyst analyses and microscopic observation and photography were conducted by IG-M and AA. Multivariate statistical analyses were performed by IG-M. All authors participated in data discussion, figure elaboration, and manuscript writing.

FUNDING

This work was a contribution to HABWAVE project LISBOA-01-0145-FEDER-031265, co-funded by EU ERDF funds, within the PT2020 Partnership Agreement and Compete 2020, and national funds through Fundação para a Ciência e Tecnologia, I.P.(FCT, I.P.) and FCT, I.P. under the project UIDB/04292/2020, and also to AQUIMAR project MAR2020 No. MAR-02.01.01-FEAMP-017. This work was also supported by funding from the European Union's Horizon 2020 Research and Innovation Programme under grant agreement N 810139: Project Portugal Twinning for Innovation and Excellence in Marine Science and Earth Observation – PORTWIMS. IG-M was supported by a postdoctoral fellowship from Xunta de Galicia, Spain (ref. ED481B-2019-074, 2019).

ACKNOWLEDGMENTS

Teresa Moita (CCMAR – Centro de Ciências do Mar, Universidade do Algarve, Portugal) is greatly acknowledged for her invaluable help in the preparation of the distribution maps. We also thank Melissa Hatherly for her great assintance in the processing of sediment samples for cyst analyses. We are grateful to all the researchers, students and the crew of "N. O. Auriga", who were most helpful in ensuring the success of the cruise, and especially to Raquel Melo for her technical assistance on-board and geographical data base management. We also thank the reviewers for their comments which greatly improved the manuscript. This study has been conducted using E.U. Copernicus Marine Service Information and data obtained from the Physical Oceanography Distributed Active Archive Centre (PO.DAAC) at JPL (Jet Propulsion Laboratory).

SUPPLEMENTARY MATERIAL

The Supplementary Material for this article can be found online at: https://www.frontiersin.org/articles/10.3389/fmars.2021.699483/full#supplementary-material

Supplementary Plate 1 | Photomicrographs of selected dinoflagellate cysts from sediment samples off Aveiro-Figueira da Foz (Atlantic Iberian margin): (1–4) cf. *Ensiculifera tyrrhenica* (sensu Li et al., 2020), sample B46: (1–2) Phase-contrast images, (3–4) bright-field images. Bright-field images: (5) *Protoceratium reticulatum*, B64; (6) full cyst of *Spiniferites* cf. *membranaceus*, B64; (7) *Spiniferites mirabilis,* B88; (8) *Protoperidinium shanghaiense*, B64; (9) *Impagidinium aculeatum,* B64; (10) *Polykrikos kofoidii* (sensu Matsuoka et al., 2009), B15; (11) *Protoperidinium conicum*, B15; and (12) *Echinidinium transparantum*, B64.

Supplementary Plate 2 | Bright-field photomicrographs of selected dinoflagellate cysts from sediment samples off Aveiro-Figueira da Foz (Atlantic Iberian margin): (1) *Protoperidinium divaricatum*, B84; (2) *Gymnodinium catenatum,* B64; (3) *Gymnodinium microreticulatum,* B64; (4) *Protoperidinium avellana,* B15; (5) *Protoperidinium americanum,* B64; (6) *Quinquecuspis concreta* (cf. *Protoperidinium leonis),* B83; (7) *Lejeunecysta* cf. *sabrina,* B82; (8) *Lejeunecysta oliva,* B79; (9) *Protoperidinium subinerme,* B82; (10) *Votadinium calvum,* B64; (11) *Dubridinium* sp., B64; and (12) *Preperidinium meunieri,* B51.

REFERENCES

Abrantes, F., and Moita, M. T. (1999). Water column and recent sediment data on diatoms and coccolithophorids, off Portugal, confirm sediment record of upwelling events. *Oceanol. Acta* 22, 319–336. doi: 10.1016/s0399-1784(99)80055-3

Amorim, A. (2001). *Dinoflagellate Cyst Distribution Along the Coast of Portugal*. [Ph. D Thesis]. Lisbon: University of Lisbon.

Amorim, A., and Dale, B. (2006). Historical cyst record as evidence for the recent introduction of the dinoflagellate *Gymnodinium catenatum* in the North-Eastern Atlantic. *Afr. J. Mar. Sci.* 28, 193–197. doi: 10.2989/18142320609504146

Amorim, A., Dale, B., Godinho, R., and Brotas, V. (2002). *Gymnodinium catenatum*-like cysts (Dinophyceae) in recent sediments from the coast of Portugal. *Phycologia* 40, 572–582. doi: 10.2216/i0031-8884-40-6-572.1

Amorim, A., Moita, M. T., and Oliveira, P. (2004). "Dinoflagellate blooms related to coastal upwelling plumes off Portugal," in *Harmful Algae 2002*, eds K. A. Steidinger, J. H. Landsberg, C. R. Tomas, and G. A. Vargo (St. Petersburg, FL: Florida Fish and Wildlife Conservation Commission), 89–91.

Amorim, A., Palma, A. S., Sampayo, M. A., and Moita, M. T. (2001). "On a *Lingulodinium polyedrum* bloom in Setúbal Bay, Portugal," in *Harmful Algal Blooms 2000*, eds G. M. Hallegraeff, S. I. Blackburn, C. J. Bolch, and R. J. Lewis (Paris: Intergovernmental Oceanographic Commission of UNESCO), 133–136.

Anderson, D. M., Stock, C. A., Keafer, B. A., Nelson, A. B., Thompson, B., McGillicuddy, D. J. Jr., et al. (2005). *Alexandrium fundyense* cyst dynamics in the Gulf of Maine. *Deep Sea Res. II Top. Stud. Oceanogr.* 52, 2522–2542. doi: 10.1016/j.dsr2.2005.06.014

Berdalet, E., Montresor, M., Reguera, B., Roy, S., Yamazaki, H., Cembella, A., et al. (2017). Harmful algal blooms in fjords, coastal embayments, and stratified systems: recent progress and future research. *Oceanography* 30, 46–57. doi: 10.5670/oceanog.2017.109

Blanco, J. (1995). The distribution of dinoflagellate cysts along the Galician (NW Spain) coast. *J. Plankton Res.* 17, 283–302. doi: 10.1093/plankt/17.2.283

Bolch, C. J. S. (1997). The use of sodium polytungstate for the separation and concentration of living dinoflagellate cysts from marine sediments. *Phycologia* 36, 472–478. doi: 10.2216/i0031-8884-36-6-472.1

Bravo, I., and Figueroa, R. I. (2014). Towards an ecological understanding of dinoflagellate cyst functions. *Microorganisms* 2, 11–32. doi: 10.3390/microorganisms2010011

Bravo, I., Fraga, S., Figueroa, R. I., Pazos, Y., Massanet, A., and Ramilo, I. (2010). Bloom dynamics and life cycle strategies of two toxic dinoflagellates in a coastal upwelling system (NW Iberian Peninsula). *Deep Sea Res. II Top. Stud. Oceanogr.* 57, 222–234. doi: 10.1016/j.dsr2.2009.09.004

Bringué, M., Pospelova, V., and Field, D. B. (2014). High resolution sedimentary record of dinoflagellate cysts reflects decadal variability and 20th century warming in the Santa Barbara Basin. *Quat. Sci. Rev.* 105, 86–101. doi: 10.1016/j.quascirev.2014.09.022

Bringué, M., Pospelova, V., and Pak, D. (2013). Seasonal production of organic-walled dinoflagellate cysts in an upwelling system: a sediment trap study from the Santa Barbara Basin, California. *Mar. Micropaleontol.* 100, 34–51. doi: 10.1016/j.marmicro.2013.03.007

Brosnahan, M. L., Fischer, A. D., Lopez, C. B., Moore, S. K., and Anderson, D. M. (2020). Cyst-forming dinoflagellates in a warming climate. *Harmful Algae* 91:101728. doi: 10.1016/j.hal.2019.101728

Chin, T. M., Vazquez-Cuervo, J., and Armstrong, E. M. (2017). A multi-scale high-resolution analysis of global sea surface temperature. *Remote Sens. Environ.* 200, 154–169. doi: 10.1016/j.rse.2017.07.029

Cordeiro, N. G. F., Nolasco, R., Cordeiro-Pires, A., Barton, E. D., and Dubert, J. (2015). Filaments on the Western Iberian Margin: a modeling study. *JGR Oceans* 120, 5400–5416. doi: 10.1002/2014jc010688

Cunha, P. P., and Dinis, J. (2002). "Sedimentary dynamics of the mondego estuary," in *Aquatic Ecology of the Mondego River Basinglobal Importance of Local Experience*, eds M. A. Pardal, M. A. S. Graça, and J. C. Marques Coimbra (Portugal: Imprensa da Universidade de Coimbra), 43–63. doi: 10.14195/978-989-26-0336-0_4

Da Silva, J. F., and Oliveira, F. (2007). "The eutrophication in the River Vouga basin–impacts on the quality of water for public supply," in *Proceedings of the Fourth Inter-Celtic Colloquium on Hidrology and Management of Water Resources, Guimarães, Portugal, July 2005. IAHS Publication Series. Water in Celtic Countries: Quantity, Quality and Climate Variability*, Vol. 310, Guimarães, 139–147.

Dale, B. (1976). Cyst formation, sedimentation, and preservation: factors affecting dinoflagellate assemblages in recent sediments from Trondhheimsfjord, Norway. *Rev. Palaeobot. Palynol.* 22, 39–60.

Dale, B. (1996). "Dinoflagellate cyst ecology: modeling and geological applications," in *Palynology: Principles and Applications*, eds J. Jansonius and D. C. McGregor (Salt Lake: Publishers Press), 1249–1275.

Dale, B., and Dale, A. (2002). "Environmental applications of dinoflagellate cysts and acritarchs," in *Quaternary Environmental Micropaleontology*, ed. S. K. Haslett (London: Arnold), 207–240.

Dale, B., Dale, A. L., and Jansen, J. H. F. (2002). Dinoflagellate cysts as environmental indicators in surface sediments from the congo deep-sea fan and adjacent regions. *Palaeogeogr. Palaeoclimatol. Palaeoecol.* 185, 309–338. doi: 10.1016/s0031-0182(02)00380-2

De Schepper, S., Ray, J. L., Skaar, K. S., Sadatzki, H., Ijaz, U. Z., Stein, R., et al. (2019). The potential of sedimentary ancient DNA for reconstructing past sea ice evolution. *ISME J.* 13, 2566–2577. doi: 10.1038/s41396-019-0457-1

de Vernal, A., Radia, T., Zaragosi, S., Van Nieuwenhove, N., Rochon, R., Allana, A., et al. (2020). Distribution of common modern dinoflagellate cyst taxa in surface sediments of the Northern Hemisphere in relation to environmental parameters: the new n=1968 database. *Mar. Micropaleontol.* 159:101796. doi: 10.1016/j.marmicro.2019.101796

Dias, J. M. A. (2004). *A Análise Sedimentar e o Conhecimento Dos Sistemas Marinhos (Uma Introdução à Oceanografia Geológica)*. Available online at: https://www.academia.edu/3170602/A_AN%C3%81LISE_SEDIMENTAR_E_O_CONHECIMENTO_DOS_SISTEMAS_MARINHOS_Uma_Introdu%C3%A7%C3%A3o_%C3%A0_Oceanografia_Geol%C3%B3gica_ (accessed November 15, 2020).

Dias, J. M. A., Gonzalez, R., Garcia, C., and Diaz-del-Rio, V. (2002). Sediment distribution patterns on the Galicia-Minho continental shelf. *Prog. Oceanogr.* 52, 215–231. doi: 10.1016/s0079-6611(02)00007-1

Dias, J. M., Lopes, J., and Dekeyser, I. (1999). Hydrological characterisation of Ria de Aveiro, Portugal, in early summer. *Oceanol. Acta* 22, 473–485. doi: 10.1016/s0399-1784(00)87681-1

Díaz, P. A., Reguera, B., Moita, T., Bravo, I., Ruiz-Villarreal, M., and Fraga, S. (2019). Mesoscale dynamics and niche segregation of two Dinophysis species in Galician-Portuguese coastal waters. *Toxins* 11:37. doi: 10.3390/toxins11010037

Ellegaard, M., and Ribeiro, S. (2018). The long−term persistence of phytoplankton resting stages in aquatic 'seed banks'. *Biol. Rev.* 93, 166–183. doi: 10.1111/brv.12338

Ellegaard, M., Dale, B., Mertens, K. N., Pospelova, V., and Ribeiro, S. (2017). "Dinoflagellate cysts as proxies for Holocene and recent environmental change in estuaries: diversity, abundance and morphology," in *Application of Paleoenvironmental Techniques in Estuarine Studies, Developments in Paleoenvironmental Research 20*, eds K. Weckström, K. Saunders, P. A. Gell, and C. Skilbeck (Berlin: Springer), 295–312. doi: 10.1007/978-94-024-0990-1_12

Elshanawany, R., and Zonneveld, K. A. (2016). Dinoflagellate cyst distribution in the oligotrophic environments of the Gulf of Aqaba and northern Red Sea. *Mar. Micropaleontol.* 124, 29–44.

NP EN933-1 (2014). *Ensaios das Propriedades Geométricas dos Agregados; Parte 1: Análise Granulométrcia; Método da Peneiração*. Caparica: Norma Portuguesa, Instituto Português da Qualidade.

Falkowski, P. G., and Knoll, A. H. (2007). "An introduction to primary producers in the sea: who they are, what they do, and when they evolved," in *Evolution of Primary Producers in the Sea*, eds P. G. Falkowski and A. H. Knoll (London: Elsevier Academic Press), 1–6. doi: 10.1016/b978-012370518-1/50002-3

Fernández-Nóvoa, D., deCastro, M., Des, M., Costoya, X., Mendes, R., and Gómez-Gesteira, M. (2017). Characterization of Iberian turbid plumes by means of synoptic patterns obtained through MODIS imagery. *J. Sea Res.* 126, 12–25. doi: 10.1016/j.seares.2017.06.013

Fiúza, A. F. G. (1983). "Upwelling patterns off Portugal," in *Coastal Upwelling, its Sediment Record*, eds E. Suess and J. Thiede (New York, NY: Plenum Publishing), 85–98. doi: 10.1007/978-1-4615-6651-9_5

Fiúza, A. F. G., Macedo, M. E., and Guerreiro, M. R. (1982). Climatological space and time variation of the Portuguese coastal upwelling. *Oceanol. Acta* 5, 31–50.

Folk, R. L. (1974). *The Petrology of Sedimentary Rocks*. Austin, TX: Hemphill Publishing Co.

Fraga, S., Anderson, D. M., Bravo, I., Reguera, B., Steidinger, K. A., and Yentsch, C. M. (1988). Influence of upwelling relaxation on dinoflagellates and shellfish toxicity in Ria de Vigo, Spain. *Estuar. Coast. Shelf Sci.* 27, 349–361. doi: 10.1016/0272-7714(88)90093-5

Fraga, S., Bravo, I., and Reguera, B. (1993). "Poleward surface current at the shelf break and blooms of *Gymnodinium catenatum* in Ria de Vigo (NW Spain)," in *Toxic Phytoplankton Blooms in the Sea*, eds T. J. Samyda and Y. Shimizu (Amsterdam: Elsevier Science Publications), 245–249.

García-Moreiras, I., Pospelova, V., García-Gil, S., and Muñoz Sobrino, C. (2018). Climatic and anthropogenic impacts on the Ría de Vigo (NW Iberia) over the last two centuries: a high-resolution dinoflagellate cyst sedimentary record. *Palaeogeogr. Palaeoclimatol. Palaeoecol.* 504, 201–218. doi: 10.1016/j.palaeo.2018.05.032

García-Moreiras, I., Sanchez, J. M., and Muñoz Sobrino, C. (2015). Modern pollen and nonpollen palynomorph assemblages of salt marsh and subtidal environments from the Ría de Vigo (NW Iberia). *Rev. Palaeobot. Palynol.* 219, 157–171. doi: 10.1016/j.revpalbo.2015.04.006

García-Moreiras, I., Delgado, C., Martínez-Carreño, N., García-Gil, S., and Muñoz Sobrino, C. (2019). Climate and vegetation changes in coastal ecosystems during the Middle Pleniglacial and the early Holocene: two multi-proxy, high-resolution records from Ría de Vigo (NW Iberia). *Glob. Planet. Chang.* 176, 100–122. doi: 10.1016/j.gloplacha.2019.02.015

Gurdebeke, P., Mertens, K. N., Pospelova, V., Matsuoka, K., Li, Z., Gribble, K. E., et al. (2019). Taxonomic revision, phylogeny, and cyst wall composition of the dinoflagellate cyst genus Votadinium Reid (Dinophyceae, Peridiniales, Protoperidiniaceae). *Palynology* 44, 310–335. doi: 10.1080/01916122.2019.1580627

Hallegraeff, G. M., Anderson, D. M., and Cembella, A. D. (2003). *Manual on Harmful Marine Microalgae*. Paris: UNESCO Publishing.

Hansen, P. J. (2011). The role of photosynthesis and food uptake for the growth of marine mixotrophic dinoflagellates.". *In J. Eukaryot. Microbiol.* 5, 203–214. doi: 10.1111/j.1550-7408.2011.00537.x

Haynes, R., Barton, E. D., and Pilling, I. (1993). Development, persistence, and variability of upwelling filaments off the Atlantic coast of the Iberian Peninsula. *J. Geophys. Res.* 98, 22681–22692. doi: 10.1029/93jc02016

Head, M. J. (1996). "Modern dinoflagellate cysts and their biological affinities," in *Palynology: Principles and Applications*, Vol. 3, eds J. Jansonius and D. C. McGregor (Dallas: AASP Foundation), 1197–1248.

International Organization for Standardization [ISO] (2009). *ISO 13320:2009: Particle size Analysis. Laser Diffraction Methods*. Geneva: ISO.

Jouanneau, J. M., Weber, O., Drago, T., Rodrigues, A., Oliveira, A., Dias, J. M. A., et al. (2002). Recent sedimentation and sedimentary budgets on the western Iberian shelf. *Prog. Oceanogr.* 52, 261–275. doi: 10.1016/s0079-6611(02)00010-1

JPL (2015). *JPL Mur Measures Project. Ghrsst Level 4 MUR Global Foundation Sea Surface Temperature Analysis. Ver. 4.1. PO.DAAC, CA, USA*. Available online at: https://doi.org/10.5067/GHGMR-4FJ04. (Accessed October, 1, 2020).

Leroy, S. A. G., Lahijani, H. A. K., Reyss, J.-L., Chalié, F., Haghani, S., Shah-Hosseini, M., et al. (2013). A two-step expansion of the dinocyst *Lingulodinium machaerophorum* in the Caspian Sea: the role of changing environment. *Quat. Sci. Rev.* 77, 31–45. doi: 10.1016/j.quascirev.2013.06.026

Lewis, J., and Hallett, R. (1997). *Lingulodinium polyedrum* (Gonyaulax polyedra) a blooming dinoflagellate. *Oceanogr. Mar. Biol.* 35, 97–161.

Li, Z., Mertens, K. N., Gottschling, M., Gu, H., Söohner, S., Price, A. M., et al. (2020). Taxonomy and molecular phylogenetics of ensiculiferaceae, fam. nov. (Peridiniales, Dinophyceae), with consideration of their life-history. *Protist* 171:125759. doi: 10.1016/j.protis.2020.125759

Loureiro, S., Reñé, A., Garcés, E., Camp, J., and Vaqué, D. (2011). Harmful algal blooms (HABs), dissolved organic matter (DOM), and planktonic microbial community dynamics at a near-shore and a harbour station influenced by upwelling (SW Iberian Peninsula). *J. Sea Res.* 65, 401–413. doi: 10.1016/j.seares.2011.03.004

Lundholm, N., Ribeiro, S., Andersen, T. J., Koch, T., Godhe, A., Ekelund, F., et al. (2011). Buried alive – germination of up to a century-old marine protist resting stages. *Phycologia* 50, 629–640. doi: 10.2216/11-16.1

Luo, Z., Mertens, K. N., Nézan, E., Gu, L., Pospelova, V., Thoha, H., et al. (2019). Morphology, ultrastructure and molecular phylogeny of cyst-producing Caladoa arcachonensis gen. et sp. nov. (Peridiniales, Dinophyceae) from France and Indonesia. *Eur. J. Phycol.* 54, 235–248. doi: 10.1080/09670262.2018.1558287

Marret, F., and Zonneveld, K. A. F. (2003). Atlas of modern organic-walled dinoflagellate cyst distribution. *Rev. Palaeobot. Palynol.* 125, 1–200.

Marques, J. C., Graça, M. A. S., and Pardal, M. A. (2002). "Introducing the Mondego river basin," in *Aquatic Ecology of the Mondego River Basin Global Importance of Local Experience*, eds M. A. Pardal, M. A. S. Graça, and J. C. Marques (Coimbra: Imprensa da Universidade de Coimbra), 7–12. doi: 10.14195/978-989-26-0336-0_1

Marret, F., Bradley, L., de Vernal, A., Hardy, W., Kim, S. Y., Mudie, P., et al. (2020). From bi-polar to regional distribution of modern dinoflagellate cysts, an overview of their biogeography. *Mar. Micropaleontol.* 159:101753. doi: 10.1016/j.marmicro.2019.101753

Matsuoka, K., and Head, M. J. (2013). "Clarifying cyst-motile stage relationships in dinoflagellates," in *Biological and Geological Perspectives of Dinoflagellates*, eds J. M. Lewis, F. Marret, and L. Bradley (London: The Micropalaeontological Society), 325–350. doi: 10.1144/tms5.31

Matsuoka, K., Kawami, H., Nagai, S., Iwataki, M., and Takayama, H. (2009). Re-examination of cyst-motile relationships of *Polykrikos kofoidii* Chatton and *Polykrikos schwartzii* Butschli (Gymnodiniales, Dinophyceae). *Rev. Palaeobot. Palynol.* 154, 79–90. doi: 10.1016/j.revpalbo.2008.12.013

McMannus, J. (1988). "Grain size determination and interpretation," in *Techniques in Sedimentology*, ed. M. Tucker (Oxford: Blackwell Scientific Publications), 63–85.

Mertens, K. N., Gu, H., Gurdebeke, P. R., Takano, Y., Clarke, D., Aydin, H., et al. (2020). A review of rare, poorly known, and morphologically problematic extant marine organic-walled dinoflagellate cyst taxa of the orders Gymnodiniales and Peridiniales from the Northern Hemisphere. *Mar. Micropaleontol.* 159:101773. doi: 10.1016/j.marmicro.2019.101773

Moita, M. T. (2001). *Estrutura, Variabilidade e Dinâmica do Fitoplâncton Nacosta de Portugal Continental*. [PhD Thesis]. Lisboa: Universidade de Lisboa.

Moita, M. T., Oliveira, P. B., Mendes, J. C., and Palma, A. S. (2003). Distribution of chlorophyll a and *Gymnodinium catenatum* associated with coastal upwelling plumes off central Portugal. *Acta Oecol.* 24, S125–S132.

Moita, M. T., Vilarinho, M. G., and Palma, A. S. (1998). "On the variability of *Gymnodinium catenatum* graham blooms in portuguese waters," in *Harmful Algae*, eds B. Reguera, J. Blanco, M. L. Fernández, and T. Wyatt (Paris: Xunta de Galicia and Intergovernmental Oceanographic Commission of UNESCO), 118–121.

Montresor, M., Zingone, A., and Marino, D. (1993). The calcareous resting cyst of *Pentapharsodinium tyrrhenicum* comb. nov. (Dinophyceae). *J. Phycol.* 29, 223–230. doi: 10.1111/j.0022-3646.1993.00223.x

Oksanen, J., Blanchet, F. G., Kindt, R., Legendre, P., Minchin, P. R., O'Hara, R. B., et al. (2015). *Package 'Vegan' Community Ecology Package: Ordination, Diversity and Dissimilarities*. Available online at: http://cran.r-project.org (Accessed November, 1, 2020)

Oliveira, A., Santos, A. I., Rodrigues, A., and Vitorino, J. (2007). Sedimentary particle distribution and dynamics on the Nazaré canyon system and adjacent shelf (Portugal). *Mar. Geol.* 246, 105–122. doi: 10.1016/j.margeo.2007.04.017

Oliveira, A., Vitorino, J., and Rodrigues, A. (2001). Nepheloid layer dynamics of the northern Portuguese shelf. *Prog. Oceanogr.* 52, 195–213. doi: 10.1016/s0079-6611(02)00006-x

Oliveira, A., Vitorino, J., Rodrigues, A., Jouanneau, J. M., Dias, J. A., and Weber, O. (2002). Nepheloid layer dynamics in the northern Portuguese shelf. *Prog. Oceanogr.* 52, 195–213.

Oliveira, P. B., Amorim, F. N., Dubert, J., Nolasco, R., and Moita, T. (2019). Phytoplankton distribution and physical processes off NW Iberia during two consecutive upwelling seasons. *Cont. Shelf Res.* 190:103987. doi: 10.1016/j.csr.2019.103987

Orlova, T. Y., Morozova, T. V., Gribble, K. E., Kulis, D. M., and Anderson, D. M. (2004). Dinoflagellate cysts in recent marine sediments from the east coast of Russia. *Bot. Mar.* 47, 184–201.

Peliz, A., Rosa, T., Santos, A. M. P., and Pissara, J. L. (2002). Fronts, jets, and counter flows in the Western Iberian upwelling system. *J. Mar. Syst.* 35, 61–77. doi: 10.1016/s0924-7963(02)00076-3

Pitcher, G. C., Figueiras, F. G., Hickey, B. M., and Moita, M. T. (2010). The physical oceanography of upwelling systems and the development of harmful algal blooms. *Prog. Oceanogr.* 85, 5–32. doi: 10.1016/j.pocean.2010.02.002

Pospelova, V., de Vernal, A., and Pedersen, T. F. (2008). Distribution of dinoflagellate cysts in surface sediments from the northeastern Pacific Ocean (43–25°N) in relation to sea-surface temperature, salinity, productivity and coastal upwelling. *Mar. Micropaleontol.* 68, 21–48. doi: 10.1016/j.marmicro.2008.01.008

Price, A. M., and Pospelova, V. (2011). High-resolution sediment trap study of organic-walled dinoflagellate cyst production and biogenic silica flux in Saanich Inlet (BC, Canada). *Mar. Micropaleontol.* 80, 18–43. doi: 10.1016/j.marmicro.2011.03.003

R Development Core Team (2013). *R: A Language and Environment for Statistical Computing*. Vienna: R Foundation for Statistical Computing.

Radi, T., Bonnet, S., Cormier, M.-A., de Vernal, A., Durantou, L., Faubert, É, et al. (2013). Operational taxonomy and (paleo-)autecology of round, brown, spiny dinoflagellate cysts from the Quaternary of high northern latitudes. *Mar. Micropaleontol.* 98, 41–57. doi: 10.1016/j.marmicro.2012.11.001

Relvas, P., Barton, E. D., Dubert, J., Oliveira, P. B., Peliz, A., Da Silva, J. C. B., et al. (2007). Physical oceanography of the western Iberia ecosystem: latest views and challenges. *Prog. Oceanogr.* 74, 149–173. doi: 10.1016/j.pocean.2007.04.021

Ribeiro, S., Amorim, A., Abrantes, F., and Ellegaard, M. (2016). Environmental change in the Western Iberia upwelling ecosystem since the preindustrial period revealed by dinoflagellate cyst records. *Holocene* 26, 874–889. doi: 10.1177/0959683615622548

Ribeiro, S., Amorim, A., Andersen, T. J., Abrantes, F., and Ellegaard, M. (2012). Reconstructing the history of an invasion: the toxic phytoplankton species Gymnodinium catenatum in the Northeast Atlantic. *Biol. Invasions* 14, 969–985. doi: 10.1007/s10530-011-0132-6

Ribeiro, S., and Amorim, A. (2008). Environmental drivers of temporal succession in recent dinoflagellate cyst assemblages from a coastal site in the North-East Atlantic (Lisbon Bay, Portugal). *Mar. Micropaleontol.* 68, 156–178. doi: 10.1016/j.marmicro.2008.01.013

Schnepf, E., and Elbrächter, M. (1992). Nutritional strategies in dinoflagellates: a review with emphasis on cell biological aspects. *Eur. J. Protistol.* 28, 3–24. doi: 10.1016/s0932-4739(11)80315-9

Shepard, F. P. (1954). Nomenclature based on sand-silt-clay ratios. *J. Sediment. Res.* 24, 151–158.

Silva, T., Caeiro, M. F., Costa, P. R., and Amorim, A. (2015). *Gymnodinium catenatum* Graham isolated from the Portuguese coast: toxin content and genetic characterization. *Harmful Algae* 48, 94–104. doi: 10.1016/j.hal.2015.07.008

Smayda, T. J. (2002). Turbulence, watermass stratification and harmful algal blooms: an alternative view and frontal zones as 'pelagic seed banks.'. *Harmful Algae* 1, 95–112. doi: 10.1016/s1568-9883(02)00010-0

Smayda, T. J. (2010). Adaptations and selection of harmful and other dinoflagellate species in upwelling systems 1. morphology and adaptive polymorphism. *Prog. Oceanogr.* 85, 53–70. doi: 10.1016/j.pocean.2010.02.004

Smayda, T. J., and Reynolds, C. S. (2001). Community assembly in marine phytoplankton: application of recent models to harmful dinoflagellate blooms. *J. Plankton Res.* 23, 447–461. doi: 10.1093/plankt/23.5.447

Smayda, T. J., and Reynolds, C. S. (2003). Strategies of marine dinoflagellate survival and some rules of assembly. *J. Sea Res.* 49, 95–106. doi: 10.1016/s1385-1101(02)00219-8

Smayda, T. J., and Trainer, V. L. (2010). Dinoflagellate blooms in upwelling systems: seeding, variability, and contrasts with diatom bloom behaviour. *Prog. Oceanogr.* 85, 92–107. doi: 10.1016/j.pocean.2010.02.006

Sordo, I., Barton, E. D., Cotos, J. M., and Pazos, Y. (2001). An inshore poleward current in the nw of the iberian peninsula detected from satellite images, and its relation with *G. catenatum* and *D. acuminata* blooms in the Galician Rias. *Estuar. Coast. Shelf Sci.* 53, 787–799. doi: 10.1006/ecss.2000.0788

Sotillo, M. G., Cailleau, S., Lorente, P., Levier, B., Aznar, R., Reffray, G., et al. (2015). The myocean IBI ocean forecast and reanalysis systems: operational products and roadmap to the future copernicus service. *J. Operat. Oceanogr.* 8, 1–18.

Sousa, F. M., and Bricaud, A. (1992). Satellite -derived phytoplankton pigment structures in the Portuguese upwelling area. *J. Geophys. Res.* 97, 11343–11356. doi: 10.1029/92jc00786

Sprangers, M., Dammers, N., Brinkhuis, H., van Weering, T. C. E., and Lotter, A. F. (2004). Modern organic-walled dinoflagellate cyst distribution offshore NWIberia; tracing the upwelling system. *Rev. Palaeobot. Palynol.* 128, 97–106. doi: 10.1016/s0034-6667(03)00114-3

Stoecker, D. K., Hansen, P. J., Caron, D. A., and Mitra, A. (2017). Mixotrophy in the marine plankton. *Annu. Rev. Mar. Sci.* 9, 311–335. doi: 10.1146/annurev-marine-010816-060617

Susek, E., Zonneveld, K. A. F., Fischer, G., Versteegh, G. J. M., and Willems, H. (2005). Organic-walled dinoflagellate cyst production in relation to upwelling intensity and lithogenic influx in the Cape Blanc region (off north-west Africa). *Phycol. Res.* 53, 97–112. doi: 10.1111/j.1440-183.2005.00377.x

ter Braak, C. J. F., and Prentice, I. C. (1988). A theory of gradient analysis. *Adv. Ecol. Res.* 18, 271–313.

Vale, P., Botelho, M. J., Rodrigues, S. M., Gomes, S. S., and Sampayo, M. A. M. (2008). Two decades of marine biotoxin monitoring in bivalves from Portugal (1986-2006): a review of exposure assessment. *Harmful Algae* 7, 11–25. doi: 10.1016/j.hal.2007.05.002

Van Nieuwenhove, N., Head, M. J., Limoges, A., Pospelova, V., Mertens, K. N., Matthiessen, J., et al. (2020). An overview and brief description of common marine organic-walled dinoflagellate cyst taxa occurring in surface sediments of the Northern Hemisphere. *Mar. Micropaleontol.* 159:101814. doi: 10.1016/j.marmicro.2019.101814

Villamaña, M., Mouriño−Carballido, B., Maranón, E., Cermeno, P., Choucino, P., da Silva, J. C. B., et al. (2017). Role of internal waves on mixing, nutrient supply and phytoplankton community structure during spring and neap tides in the upwelling ecosystem of Ría de Vigo (NW Iberian Peninsula). *Limnol. Oceanogr.* 62, 1014–1030. doi: 10.1002/lno.10482

Vitorino, J. P. N. (1989). Circulacão residual ao largo da costa NW de Portugal durante o afloramento de 1987. *Anais Inst. Hidrogr.* 10, 25–37.

Wall, D., and Dale, B. (1966). "Living fossils" in western Atlantic plankton. *Nature* 211, 1025–1026. doi: 10.1038/2111025a0

Wall, D., and Dale, B. (1968). Quaternary calcareous dinoflagellates (Calciodinellideae) and their natural affinities. *J. Paleonto.* l42, 1395–1408.

Wall, D., Dale, B., Lohmann, G. P., and Smith, W. K. (1977). The environmental and climatic distribution of dinoflagellate cysts in modern marine sediments from regions in the North and South Atlantic oceans and adjacent seas. *Mar. Micropaleontol.* 2, 121–200. doi: 10.1016/0377-8398(77)90008-1

Wang, N., Mertens, K. N., Krock, B., Luo, Z., Derrien, A., Pospelova, V., et al. (2019). Cryptic speciation in *Protoceratium reticulatum* (Dinophyceae): evidence from morphological, molecular and ecophysiological data. *Harmful Algae* 88:101610. doi: 10.1016/j.hal.2019.05.003

Wells, M. L., Trainer, V. L., Smayda, T. J., Karlson, B. S. O., Trick, C. G., Kudela, R. M., et al. (2015). Harmful algal blooms and climate change: learning from the past and present to forecast the future. *Harmful Algae* 49, 68–93. doi: 10.1016/j.hal.2015.07.009

Wentworth, C. K. (1922). A scale of grade and class terms for clastic sediments. *J. Geol.* 30, 377–392. doi: 10.1086/622910

Zonneveld, K. A. F., and Brummer, G.-J. A. (2000). (Palaeo-)ecological significance, transport and preservation of organic-walled dinoflagellate cysts in the Somali Basin, NW Arabian Sea. *Deep Sea Res. II Top. Stud. Oceanogr.* 47, 2229–2256. doi: 10.1016/s0967-0645(00)00023-0

Zonneveld, K. A. F., and Pospelova, V. (2015). A determination key for modern dinoflagellate cysts. *Palynology* 39, 387–409. doi: 10.1080/01916122.2014.990115

Zonneveld, K. A. F., Chen, L., and Möbius, L. (2009). Environmental significance of dinoflagellate cysts from the proximal part of the Po-river discharge plume (off southern Italy, Eastern Mediterranean). *J. Sea Res.* 2, 189–213. doi: 10.1016/j.seares.2009.02.003

Zonneveld, K. A. F., Ebersbach, F., Maeke, M., and Versteegh, G. J. (2018). Transport of organic-walled dinoflagellate cysts in nepheloid layers off Cape Blanc (NW Africa). *Deep Sea Res. I Top. Stud. Oceanogr.* 139, 55–67. doi: 10.1016/j.dsr.2018.06.003

Zonneveld, K. A. F., Marret, F., Versteegh, G. J. M., Bogus, K., Bonnet, S., Bouimetarhan, I., et al. (2013). Atlas of modern dinoflagellate cyst distribution based on 2405 data points. *Rev. Palaeobot. Palynol.* 191, 1–197. doi: 10.1016/s0034-6667(02)00229-4

Conflict of Interest: The authors declare that the research was conducted in the absence of any commercial or financial relationships that could be construed as a potential conflict of interest.